Arctic Science

OPEN ACCESS | Research Article

# Modelling permafrost distribution using the temperature at top of permafrost model in the boreal forest environment of Whatì, NT

**Scott Vegter**[a], **Philip P. Bonnaventure**[a], **Seamus Daly**[a], **and Will Kochtitzky**[b,c,d]

[a]Department of Geography and Environment, University of Lethbridge, Lethbridge, AB T1K 3M4, Canada; [b]Climate Change Institute, University of Maine, Orono, ME, USA; [c]Department of Geography, Environment and Geomatics, University of Ottawa, Ottawa, ON, Canada; [d]School of Marine and Environmental Programs, University of New England, Biddeford, ME, USA

Corresponding author: **Philip P. Bonnaventure** (email: Philip.bonnaventure@uleth.ca)



## Abstract

Current permafrost models in Canadian boreal forests are generally of low spatial resolution as they cover regional or continental scales. This study aims to understand the viability of creating a temperature at the top of permafrost (TTOP) model on a local scale in the boreal wetland environment of Whatì, Northwest Territories from short-term field-collected temperature data. The model utilizes independent variables of vegetation, topographic position index, and elevation, with the dependent variables being ground surface temperature collected from 60 ground temperature nodes and 1.5 m air temperature collected from 10 temperature stations. In doing this, the study investigates the relationship vegetation and disturbance have on ground temperature and permafrost distribution. The model predicts that 31% of the ground is underlain by permafrost, based on a mean annual temperature at TTOP of <0 °C. This model shows an accuracy of 62.5% when compared to cryotic assessment sites (CAS). Most inaccuracies, showing the limitations of the TTOP model, came from peat plateaus that had been burned in the most recent forest fire in 2014. These resulted in out-of-equilibrium permafrost and climatic conditions that TTOP cannot handle well. Commonly, permafrost mapping places Whatì in the extensive discontinuous zone, estimating that between 50% and 90% of the ground is underlain by permafrost. The study shows that a climatically driven TTOP model calibrated with CAS can be used to illustrate ground temperature heterogeneity from short-term data in boreal forest wetland environments. However, this approach likely underestimates permafrost extent and is perhaps not the best-suited modelling choice for near-surface permafrost, which is currently out of equilibrium with the current climate.

**Key words:** TTOP, boreal, forest fire, permafrost

## Introduction

Around 80% of the world's boreal forests occur in permafrost regions, and because of the extreme climate and relatively low precipitation, these environments are very responsive to climate change (Helbig et al. 2016). Within these northern boreal forests are peat-rich wetland environments. These systems are significant to the global climate as they act as a carbon sink, containing high amounts (800 Pg) of frozen organic carbon, with the potential to store up to 75 kg C $m^{-2}$ (Apps et al. 1993). Due to the extreme climate and low precipitation, boreal forests will contribute considerably to future carbon emissions through decomposition as permafrost thaws (Apps et al. 1993; Walker et al. 2018; Stuenzi et al. 2021). Arctic amplification is the phenomenon by which temperature trends and variability are much larger in the Arctic than in the rest of the world (Serreze and Barry 2011; Casagrande et al. 2021). In addition to carbon release, thawing permafrost poses issues for both the existing environment and infrastructure, including buildings, roads, and pipelines (Doré et al. 2016). These issues are further exacerbated by natural and anthropogenic disturbances in boreal forest environments, including an increase in forest fires and new infrastructure coupled with a general lack of sufficient baseline permafrost distribution maps or thaw susceptibility (Jafarov et al. 2013; Holloway et al. 2020). As such, understanding the distribution and vulnerability of permafrost to these changes is critical for planning and hazard assessment in the north today (Etzelmüller et al. 2006).

Permafrost is difficult to quantify in terms of both thermal state and spatial extent without direct in-situ observation (Koven et al. 2013). Unlike other large elements of the cryosphere (e.g., sea ice and glaciers), permafrost extent cannot be widely mapped using optical remote sensing from satellite imagery (Duguay et al. 2005). As a result, determining permafrost attributes and mapping involves fieldwork and modelling (Lewkowicz and Ednie 2004; Etzelmüller et al. 2006; Farbrot et al. 2007; Bonnaventure and Lewkowicz 2012; Deluigi et al. 2017; Garibaldi et al. 2021). The current maps

and studies used to represent permafrost are often created at a regional or national scale and utilize climate indices as a basis for permafrost presence (Heginbottom et al. 1995; Smith and Riseborough 2002; Obu et al. 2019; O'Neill et al. 2019). These models can often be misleading when applied on a local scale due to the complex role ecosystem structure plays in permafrost distribution, especially as climate changes (Van Cleve et al. 1983; Jorgenson et al. 2013). In addition, variations in soil type, vegetation, microtopography, snow cover, and hydrology also affect local-scale permafrost distribution (Jorgenson et al. 2001; Karunaratne and Burn 2003; Fisher et al. 2016; Bonnaventure et al. 2017). Permafrost presence and stability in boreal forest regions are complex and dependent on several factors. These include climatic conditions, including air temperature and snow cover. However, landscape variability in vegetation and subsurface conditions, including soil type and texture, can be equally impactful (Smith and Riseborough 2002).

The objective of this research is to examine the usability of a climate-driven model in a boreal wetland environment. The temperature at top of permafrost (TTOP) model establishes transfer functions between mean annual air temperature (MAAT), mean annual ground surface temperature (MAGST) and TTOP based on environmental factors. This model has been widely utilized in heterogeneous High Arctic environments (Bonnaventure et al. 2017; Obu et al. 2019; Garibaldi et al. 2021). This study tests the accuracy of the commonly used TTOP model against the results of a previous model (Daly et al. 2022) and identifies weaknesses of the TTOP model specific to this environment type. Permafrost in these regions is classified as climate-driven, with occurrences associated with low MAAT (Shur and Jorgenson 2007). Transferring this model to a boreal wetland environment where permafrost can be classified as climate-driven ecosystem-modified, ecosystem-driven, or even ecosystem-protected will explore the robustness of short-term climatic inputs to drive permafrost distribution modelling. Additionally, the aim is to examine if this model is suitable to determine the spatial distribution of permafrost while providing insight into permafrost thermal state that is equivalent in accuracy to a model created using ground truthing techniques paired with environment-specific variables (Daly et al. 2022). As permafrost distribution in this environment is highly subject to ecological structure, hydrology, and disturbance, we test the hypothesis that a climatically driven model like TTOP is likely to underpredict permafrost distribution in this complex environment.

## Study area

The study area is delineated by the municipal boundary of the community of Whatì NT, an area of 60 km$^2$ approximately 165 km northwest of Yellowknife, NT (Figure 1). The community has until recently only been accessible by aircraft or winter roads but was connected to the all-season road network in November 2021.

Whatì is located on the south-eastern shore of the third largest lake in the Northwest Territories, Lac La Martre. Whatì is in a subarctic climate with cool summers and year-round precipitation according to the Köppen-Geiger climate index (Dfc) (Peel et al. 2007). This climate is primarily a result of its high latitude, continental location, and proximity to water bodies. According to Environment and Climate Change Canada, the average air temperature from 2019 to 2021 in Whatì was −5.9 °C (ClimateData.ca). The elevation of the study area ranges from 238 m asl to 282 m asl. Whatì is classified as occurring within the extensive discontinuous permafrost zone, meaning that 50%–90% of the ground is underlain by permafrost (Heginbottom et al. 1995). A recent assessment of permafrost distribution in Whatì by Daly et al. (2022) predicted that the area had 50.0% permafrost coverage that was highly controlled by ecosystem type. They found that ecosystem classes with the highest probabilities of permafrost (100%, 99.9%, 99.0%, and 71%) included coniferous forest, peat plateau burnt, peat plateau, and low-shrub organic matter, while mixed-wooded forest burnt, low-shrub clearing, and wetlands generally contained the lowest probabilities (26.1%, 30.9%, and 32.9%). Permafrost in Whatì is considered "warm", having a temperature between 0 °C and −2 °C and is classified as climate-driven, ecosystem-modified (Heginbottom et al. 1995; Henry and Smith 2001; Shur and Jorgenson 2007).

The primary species of vegetation found throughout the study area are spruce trees (*Picea*), deciduous trees such as aspen (*Populus*) and willow (*Salix*), Labrador tea (*Rhododendron*), buffaloberry (*Shepherdia*), fireweed (*Epilobium*), bearberry (*Arctostaphylos*), and mosses and lichens, including peat moss (*Sphagnum*), reindeer lichen (*Cladonia*), and feathermoss (*Ptilium*). Ecosystem types in this region can be divided into nine sections: coniferous forest, coniferous burnt, mixed-wooded forest, mixed-wooded forest burnt, peat plateau, peat plateau burnt, wetland, low-shrub organic matter, and low-shrub clearing (Daly et al. 2022). A main characteristic of boreal wetland environments is the frequent occurrence of forest fires. These fires assist with several ecosystem processes, including tree recruitment, vegetation recovery, and changes in soil moisture and thermal conductivity (Van Cleve et al. 1983; Kasischke and Turetsky 2006; Holloway et al. 2020). Whatì went through a record forest fire season in 2014. The fire stopped short of the built community due to anthropogenic and natural firebreaks (Daly et al. 2022). These burns play a large role in boreal forest permafrost thawing as they remove trees that intercept snow, creating more insulation from winter temperatures, and can remove the organic layer above the permafrost that insulates it from warm summer temperatures (Yoshikawa et al. 2002).

## Methods

### Data collection and pre-setup

A network of air and ground temperature loggers was installed in and around Whatì between 2019 and 2021. These stations were deployed to maximize the spatial coverage and sampled variability of factors influencing permafrost distribution.

Locations for all sensor types were predetermined using stratified random proportional sampling based on the proportion of each vegetation type, elevation, and topographic

**Fig. 1.** Study area extent in and around the community of Whatì, as well as the location of ground temperature nodes (GTN), microclimate stations (MCS), and Whatì weather stations (WWS). Imagery © [2017] DigitalGlobe, Inc.; base map (ESRI), map datum in NAD83.

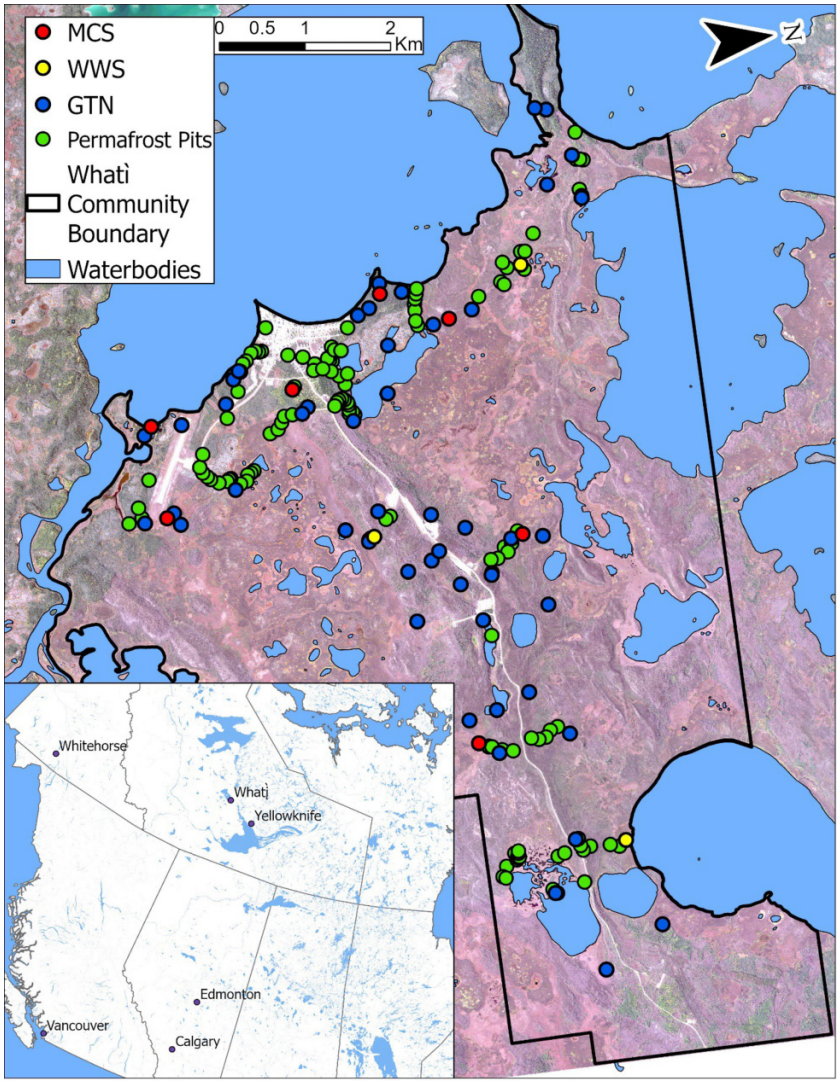




position index (TPI). In some instances, this was modified in the field due to the accessibility and accuracy of vegetation classification. The network of air sensors was installed in 2019 and consisted of seven microclimate stations (MCS) equipped with Hobo (Onset, USA) MX2301A and MX2303 loggers to collect hourly relative humidity (RH), air and ground surface temperatures, and ground temperature at a depth of 1.5 m below the surface. These loggers have an accuracy of ±0.2 °C and ±2.5% RH. Along with these, three weather stations (WWS) equipped with HOBO RX3000 measuring temperature (accuracy: ±0.2 °C), RH (±2.5%), windspeed (±1.1 m $s^{-1}$), wind direction (±5°), gust speed (±1.1 m $s^{-1}$), rain (±1%), solar radiation (±10 W $m^{-2}$), and dew point (±0.25 °C) were set up in 2019 in burnt and unburnt mixed-wooded forests, burnt and unburnt coniferous forest, and burnt and unburnt peat plateaus (Table 1).

Due to the variability of permafrost distribution outlined in Daly et al. (2022), an additional fifty ground temperature nodes (GTN) equipped with Hobo MX2201 loggers were deployed in September 2020 to measure the ground temperature every hour. These have an accuracy of ±0.5 °C and were placed 1–5 cm below the ground surface. These sites were selected using stratified random proportional sampling based on the proportional area of each vegetation type, elevation, and TPI (Table 1). Some compromises had to be made as some sites in the study area could not be accessed.

DEM-derived variables that are primarily used in permafrost studies are aspect, elevation, potential incoming solar radiation (PISR), and TPI (v. 1.3a; Jenness Enterprises 2006) (Etzelmüller et al. 2006). According to Daly et al. (2022), the low relief of the area made PISR and aspect irrelevant variables to the model, so they were not considered in ground temperature site selection. TPI refers to the elevation of a grid cell minus the mean elevation of the cells around it. TPI influences site hydrology, snow accumulation, and redistribution as hollows favour the collection of snow. The calculation of

**Table 1.** Model input variables for ground sensors including vegetation class description (Daly et al. 2022), number of sensors ($n$), number of sensors with a full year of data from 1 October 2020 to 30 September 2021 ($n = 365$), and landcover percentage of the study area.

| Variable | Class | Description | $n$ | $n$ (365) | Coverage (%) |
|---|---|---|---|---|---|
| Vegetation classification | Coniferous forest (CC) | Black spruce and tamarack tree stands with organic mat. layer including moss, lichen, Labrador tea, cinquefoil | 9 | 7 | 8.3 |
| | Coniferous forest burnt (CB) | Same as coniferous forest with grass of parnassus, sedges, and horsetails. Visible evidence of recent burn (2014) | 7 | 7 | 9.2 |
| | Mixed-wooded forest (MW) | Aspen, birch, willow, spruce, alder with thin organic mat. layer. Rose, buffalo berry, bear berry, and occasional thin layer of moss and lichen | 5 | 4 | 2.9 |
| | Mixed-wooded burnt (MWB) | Same as mixed-wood forest with fireweed. Visible evidence of recent burn (2014) | 10 | 10 | 18 |
| | Peat plateau (PP) | Visible plateau or hummocky terrain. Cloudberry, bog rosemary, white lichen, moss, Labrador tea, and spruce tree stands | 5 | 4 | 3.2 |
| | Peat plateau burnt (PPB) | Same as peat plateau with visible evidence of burn (2014) | 7 | 6 | 8.7 |
| | Wetland (WL) | Wet moss layer, grass, bog birch, fireweed, sundew, wax mertle, willow, cinquefoil, bog rosemary. High water table. Minimal resistance to soil probe | 6 | 5 | 36.5 |
| | Low-shrub organic matter (LSOM) | Coniferous forest adjacent, similar organic mat., low-density to no tree cover. Juniper, willow, spruce, Labrador tea, moss, lichen, and cinquefoil | 8 | 7 | 12.7 |
| | Low-shrub clearing (LSC) | Low-density paper birch, willow. Rose, horsetail, fireweed, and grass | 3 | 3 | 0.5 |
| Elevation | 1 | <246 m asl. | 12 | 11 | 23.3 |
| | 2 | 246–250 m asl. | 14 | 12 | 37.8 |
| | 3 | 250–255 m asl. | 20 | 17 | 24.4 |
| | 4 | 255–261 m asl. | 6 | 5 | 9.8 |
| | 5 | 261–282 m asl. | 8 | 8 | 4.6 |
| Topographic position index (TPI) | 1 | <−0.8 | 6 | 4 | 14.2 |
| | 2 | −0.8–0.0 | 24 | 22 | 33.9 |
| | 3 | 0.0–1.1 | 21 | 18 | 44.2 |
| | 4 | 1.1–8.9 | 9 | 9 | 7.7 |



TPI was taken from Daly et al. (2022), following Weiss (2001). Elevation and TPI were derived from a 2 m DEM provided by GeoEye optical imagery taken on 17 September 2017 (Imagery © [2017] DigitalGlobe, Inc.). The elevation model was produced by the Polar Geospatial Center at the University of Minnesota using surface extraction with a TIN-based search and space minimization algorithm (Noh and Howat 2017). Due to the low topographic relief of the area, elevation affects permafrost indirectly, as higher elevations in the study area are associated with more gravelly soils and larger rocks that are not conducive to the presence of permafrost, while lower elevations were observed to have more silty and loamy soils (Daly et al. 2022).

Site observations at each of the GTNs included major vegetation types, the presence of organic matter, including moss and lichen, and general substrate types. The geographic position was recorded using a handheld GPS (Garmin GPSMAP 64x series) using waypoint averaging (accuracy of 1–4 m).

Data from the GTN and MCSs were collected in October 2021 to ensure a full year of temperature data had been measured. During data collection, site observations were made for the second time to note any changes in sites from the previous year. WWS data were received biweekly via telemetry from HOBOlink.com. Air temperature data were also collected from Whatì station 1674 from the Canadian Center for Climate Services (CCCS; climatedata.ca).

## Temperature typicality

To ensure that the data were collected in a typical year, temperature typicality needs to be established for air temperature during the time data collection occurred (Garibaldi et al. 2021). This ensures that the weather in 2020 and 2021 was not an anomaly, and the findings can be compared to other studies that occurred at different times. To do this, daily average air temperature data from 1972 to 2021 was taken from the CCCS. As Whatì station 1674 was only established in 1997 and had large data gaps up until 2013, data from Yellowknife station A were used. Figure 2 shows high similarities between the monthly averages of the two stations and has an $R^2$ value

**Table 2.** Cryotic assessment sites (CAS) from Daly et al. (2022), including vegetation class, description, number of sites (*n*), number of sites containing permafrost, landcover percentage of the study area, and percentage of permafrost cover in the TTOP model.

| Variable | Class | Description | *n* | Permafrost | Coverage (%) | Permafrost extent (%) |
|---|---|---|---|---|---|---|
| Vegetation classification | Coniferous forest (CC) | Black spruce and tamarack tree stands with organic mat. layer including moss, lichen, Labrador tea, cinquefoil | 19 | 19 | 8.3 | 96 |
| | Coniferous forest burnt (CB) | Same as coniferous forest with grass of parnassus, sedges, and horsetails. Visible evidence of recent burn (2014) | 14 | 6 | 9.2 | 3.2 |
| | Mixed-wooded forest (MW) | Aspen, birch, willow, spruce, alder w/thin organic mat. layer. Rose, buffalo berry, bear berry, occasional thin layer of moss and lichen | 17 | 4 | 2.9 | 24.8 |
| | Mixed-wooded burnt (MWB) | Same as mixed-ood Forest w/fireweed. Visible evidence of recent burn (2014) | 12 | 2 | 18 | 7% |
| | Peat plateau (PP) | Visible plateau or hummocky terrain. Cloudberry, bog rosemary, white lichen, moss, Labrador tea, spruce tree stands | 16 | 16 | 3.2 | 99.7 |
| | Peat plateau burnt (PPB) | Same as peat plateau with visible evidence of burn (2014) | 26 | 26 | 8.7 | 38.3 |
| | Wetland (WL) | Wet moss layer, grass, bog birch, fireweed, sundew, wax mertle, willow, cinquefoil, bog rosemary. High water table. Minimal resistance to soil probe | 13 | 1 | 36.5 | 12.7 |
| | Low-shrub organic, matter (LSOM) | Coniferous Forest adjacent, similar organic mat., low-density to no tree cover. Juniper, willow, spruce, Labrador tea, moss, lichen, and cinquefoil | 9 | 7 | 12.7 | 71.6 |
| | Low-shrub clearing (LSC) | Low-density paper birch, willow. Rose, horsetail, fireweed, and grass | 10 | 2 | 0.5 | 4.2 |
| Elevation | 1 | <246 m asl. | 13 | 11 | 23.3 | 34.6 |
| | 2 | 246–250 m asl. | 52 | 29 | 37.8 | 23.6 |
| | 3 | 250–255 m asl. | 51 | 36 | 24.4 | 34.2 |
| | 4 | 255–261 m asl. | 20 | 7 | 9.8 | 36.2 |
| | 5 | 261–282 m asl. | 0 | 0 | 4.6 | 51.9 |
| Topographic position index (TPI) | 1 | <−0.8 | 11 | 5 | 14.2 | 27.0 |
| | 2 | −0.8–0.0 | 75 | 39 | 33.9 | 20.8 |
| | 3 | 0.0–1.1 | 47 | 37 | 44.2 | 35.8 |
| | 4 | 1.1–8.9 | 3 | 2 | 7.7 | 78.9 |



of 0.997. This station is located approximately 150 km SE of Whatì. The daily average temperature data was converted to an annual average, a 10-year average (2012–2021), and a 50-year average (1972–2021). From there, the standard deviation was calculated, and these results were compared to the 2020 and 2021 annual average temperatures.

## Temperature surfaces

### Air temperature model

Due to the low relief of the area, elevation was not considered when generating air temperature surfaces (Daly et al. 2022). To generate mean annual air temperature (MAAT), hourly data from October 2020 to September 2021 were converted to an annual average and run through an inverse distance weighting interpolation (IDW) technique in ArcGIS Pro 2.9 (ESRI, USA). Air stations that provided 365 days of data, along with the Environment and Climate Change weather station in Whatì, were used in this model.

### Ground surface temperature model

To create ground surface temperature surfaces, a multivariable linear regression model was first used to determine

**Fig. 2.** Monthly average air temperatures of Whatì station 1674 and Yellowknife station A from 2016 to 2020. The correlation has an $R^2$ value of 0.997.

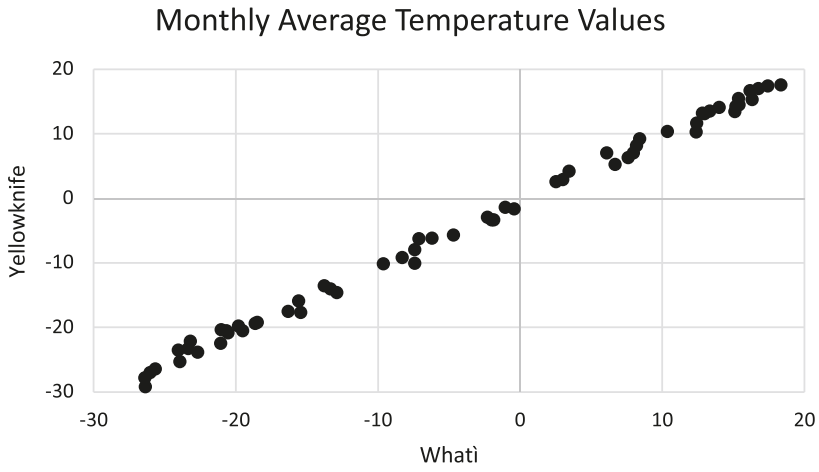




the significance between MAGST and different topographic or remote sensing variables. These variables include vegetation, TPI, elevation, and topographic wetness index (TWI). TWI was generated in ArcGIS to represent soil moisture. This was done by deriving slope, flow direction, and flow accumulation using the DEM. Elevation was used as higher elevations were composed of sandier, gravelly soils, while lower elevations became siltier (Daly et al. 2022). The TPI and elevation surfaces were reclassified using natural breaks in the data (Jenk's methods). This is a data clustering method that is designed to reduce variance within classes and maximize the variance between classes (Jenks 1967). The vegetation surface was taken from Daly et al. (2022). This surface used vegetation field observations to inform a supervised classification deriving a spatially complete vegetation map in ENVI (ENVI Version 5.5; L3 Harris Geospatial Solutions, 2008). Vegetation, TPI, and elevation had significant *p*-values less than 0.05 and therefore were the three independent variables used in the model creation and were the same variables used in Daly et al. (2022). TWI was the only variable that produced an insignificant *p*-value and was therefore removed. To generate mean annual ground surface temperature (MAGST) for the entire study area, hourly data from October 2020 to September 2021 were converted to an annual average and run through an Empirical Bayesian Kriging (EBK) regression prediction in ArcGIS Pro with the three identified independent variables. This was done on every ground station with 365 days of data.

## TTOP model

The TTOP model (eq. 1) was used in this study as a solution to calculate the temperature for both permafrost (TTOP $\leq 0$) and seasonal frost (TTOP $> 0$). The TTOP surface was created using the surfaces generated for each variable required as an input (eq. 1), where *rk* is the ratio of thawed to frozen thermal conductivity, $n_t$ and $n_f$ are the thawing and freezing *n*-factors respectively, with $TDD_a$ and $FDD_a$ being the thawing and freezing degree-days in the air, respectively, and *P* is the period (365 days).

$$(1)\quad \text{TTOP} = \frac{(rk * n_t * \text{TDD}_a) - (n_f * \text{FDD}_a)}{P} \quad \text{for TTOP} \leq 0$$

$$\text{TTOP} = \frac{(n_t * \text{TDD}_a) - \left(\frac{1}{rk} * n_f * \text{FDD}_a\right)}{P} \quad \text{for TTOP} > 0$$

## Input variables for the TTOP model

Hourly air and ground surface temperature data was collected from each of the sites in October 2021. The data were converted from hourly measurements to daily averages. Daily average ground temperature surfaces were then modelled using the EBK regression prediction, while daily average air surfaces were modelled utilizing IDW. These surfaces were then used to generate freezing and thawing degree-days for the ground surface ($FDD_g$ and $TDD_g$) and air ($FDD_a$ and $TDD_a$). These were calculated by taking the absolute summation of daily average temperatures above 0 °C for TDD and below 0 °C for FDD for October 2020 to September 2021 (Garibaldi et al. 2021). The *N*-factors were then calculated using these surfaces (eq. 2). *rk* values for each of the sites were determined using vegetation type and known, previously used *rk* values (Romanovsky and Osterkamp 1995; Smith and Riseborough 2002; Way and Lewkowicz 2016; Obu et al. 2019). These values were 0.2 for peat plateaus, 0.6 for burnt peat and wetlands, 0.3 for coniferous forests, 0.5 for burnt coniferous forests, 0.4 for low-shrub organic matter, and 0.8 for deciduous forests, burnt deciduous forest, and low-shrub clearings. In previous studies, *rk* values have proved to have little overall impact on TTOP model outputs (Garibaldi et al. 2021).). These surfaces were then all combined, following eq. 1, to generate a TTOP surface.

$$(2)\quad n_f = \frac{\text{FDD}_g}{\text{FDD}_a} \quad \text{and} \quad n_t = \frac{\text{TDD}_g}{\text{TDD}_a}$$

### Permafrost and seasonal frost solutions

The seasonal frost model was initially introduced by Smith and Riseborough (1998). To be used in conjunction with the TTOP model for areas that exhibit seasonal frost and do not have permafrost. This solution utilizes the inverse of the rk value to modify the freezing portion of the equation, correcting for the freeze/thaw state of the active layer, and generates a value above 0 °C. Most studies using the TTOP model overlook utilizing a specific seasonal frost solution strictly using the TTOP ubiquitously. As the TTOP model is meant for permafrost areas, utilizing only TTOP can lead to an underestimation of MAGT in seasonal frost areas. In areas where permafrost is discontinuous, including most boreal forest areas, this increases inaccuracies; thus, a seasonal frost model should be used. As permafrost in this region is warm, the same variables were run through an adapted seasonal frost model and permafrost model (eq. 1; TTOP > 0). The TTOP surface was then divided into areas greater than 0 °C and equal to or below 0 °C, with each model then run on their respective area as well as each for the complete area. To assess the sensitivity of the TTOP model, cells with a value between −0.5 °C and 0.5 °C were extracted from the TTOP surface, and again, both solutions were run on those cells. The same was then done for cell values between −1 °C and 1 °C.

### Accuracy assessment

To assess the accuracy of the TTOP model on permafrost distribution, the generated TTOP surface was compared to 137 out of 139 binary (permafrost present or absent) cryotic assessment sites (CAS) produced by Daly et al. (2022). CAS determined the presence or absence of near-surface permafrost using a thermal probe equipped with four thermistor cables (E348-TMC6-HD, accuracy: <±0.2 °C, resolution: <±0.03 °C). Thermistor sensors were spaced at 0, 25, and 50 cm from the maximum depth (bottom of the probe), with one additional thermistor used to measure the ground surface temperature. If the generated TTOP surface had a temperature of less than 0 °C at a CAS where permafrost was determined to be present, the site was assessed to be correct. A site was also deemed to be correct if the generated TTOP surface had a temperature greater than 0 °C with no permafrost present at the CAS. False positives occurred where the TTOP temperature was less than 0 °C at a CAS where no permafrost was present, and false negatives occurred at sites where the TTOP temperature was greater than 0 °C and permafrost was present at the CAS.

## Results

### Temperature typicality

The mean annual air temperature in Yellowknife from 1970 to 2019 was −4.2 °C with a standard deviation of 1.3 °C. The temperature range for the 50 years was −7.1 °C (1982) to −1.1 °C (1998). During the 10-year period (2012–2021), it was warmer with an average of −3.9 °C and a standard deviation of 0.9 °C. Average temperatures for 2020 and 2021 were −4.9 °C and −4.5 °C. This falls within the 50-year standard deviation of 1.3 °C. For the 10-year average, 2020 was within the standard deviation, but 2021 was outside by 0.1 °C. The mean annual precipitation for the 10-year period (2012–2021) was an average of 258.6 mm with a standard deviation of 48.7 mm. 42% of precipitation falls as snow. The study period of 1 October 2020–30 September 2021 was drier than the 10-year average, with a total precipitation of 202 mm and 46% falling as snow.

### Field results

Out of the 10 air temperature sensors, 6 recorded a full year of data from 1 October 2020 to 31 September 2021, with a MAAT of −5.3 °C and a range of −5 °C to −5.4 °C. This is 0.7 °C warmer than the Whatì Environment and Climate Change station MAAT of −6.0 °C. This places Whatì within the widespread discontinuous permafrost zone (Heginbottom et al. 1995; Smith and Riseborough 2002). Out of the 60 total ground surface temperature sensors, 53 recorded a full year of data. This included 48 GTNs, three weather stations, and two microclimate stations. The MAGST of these 53 sensors was 1.5 °C, with a range of −2.2 °C to 4.1 °C.

### Ground surface temperature

The classes with the lowest MAGST were mix-wooded forest (0.2 °C), coniferous forest (0.4 °C), and peat plateau (0.5 °C). The highest temperatures were seen in the wetland (2.8 °C), low-shrub organic matter (2.1 °C), peat plateaus burnt (1.9 °C), and low-shrub clearing (1.9 °C). In the middle are coniferous forest burnt (1.7 °C) and mix-wooded forest burnt (1.8 °C). For daily average ground surface temperature, mixed-wooded forest burnt had the largest range of values with a maximum of 17 °C and a minimum of −8 °C. Ecosystems with low organic matter, such as mixed-wooded forest burnt, low-shrub clearing, and wetlands, had the largest annual range of daily average ground temperatures (25.2 °C, 23.6 °C, and 22.9 °C). Conversely, ecosystems with high organic matter content, such as coniferous forest burnt, coniferous forest, peat plateau, and peat plateau burnt had the lowest annual range of temperatures (19.6 °C, 19.9 °C, 20.4 °C, and 20.4 °C) (Fig. 3).

Calculating cumulative FDD shows the lag in cooling between the air and ground surface temperatures (Fig. 4). Cumulative FDDg ranged from a low of 176.3 °C.days at GTN 02 in the wetland to a maximum of 1957.1 °C.days at GTN 13 in the mixed wooded forest ecoregion. On average, the lowest FDD values occurred in low shrub organic matter (441.4) and the highest occurred in mixed-wooded forests (1001.6). Lower FDDg values can be associated with greater amounts of snow and organic matter, whereas higher FDD is associated with lower snow and less organic matter (Goodrich 1982; Jorgenson and Osterkamp 2005). Cumulative thawing degree days show the differences in ground and air temperatures. Cumulative TDDg ranged from a low of 449.1 °C.days at GTN 19 in the coniferous forest burnt to a maximum of 1795.4 °C.days at GTN 34 in the mixed-wooded forest burnt. On average, the lowest TDD values occurred in coniferous forests (919.7) and the highest occurred in mixed-wooded forests burnt (1501.8) (Fig. 4). Higher TDD values indicate lower amounts of organic matter and vegetation cover.

**Fig. 3.** Box and whisker plots showing MAGST ranges of all surface sensors, mean (x), median (–), and outliers for each vegetation and meteorological seasons. (A) Fall from 1 October to 30 November 2020, and 1 to 30 September 2021. (B) Winter from 1 December 2020, to 28 February 2021. (C) Spring from 1 March to 31 May 2021. (D) Summer from 1 June to 31 August 2021. CC, coniferous forest; CB, coniferous forest burnt; MW, mixed-wooded forest; MWB, mixed-wooded forest burnt; PP, peat plateau; PPB, peat plateau burnt; LSOM, low-shrub organic matter; LSC, low-shrub clearing; and WL, wetland.

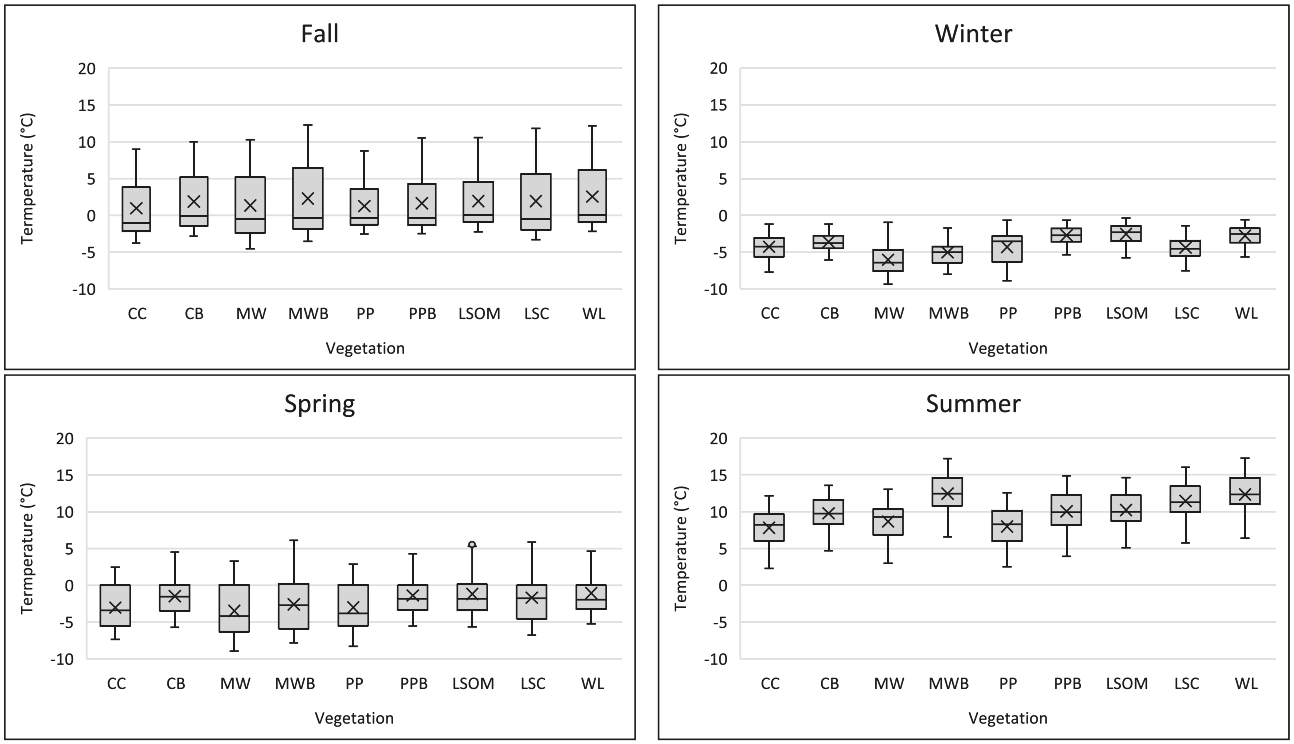


**Fig. 4.** Measured cumulative freezing and thawing degree-days (°C.days) for all vegetation classes and one air temperature station, WWS3 (red). Higher FDD values indicate less organic matter and lower snow cover. CC, coniferous forest; CB, coniferous forest burnt; MW, mixed-wooded forest; MWB, mixed-wooded forest burnt; PP, peat plateau; PPB, peat plateau burnt; LSOM, low-shrub organic matter; LSC, low-shrub clearing; and WL, wetland.

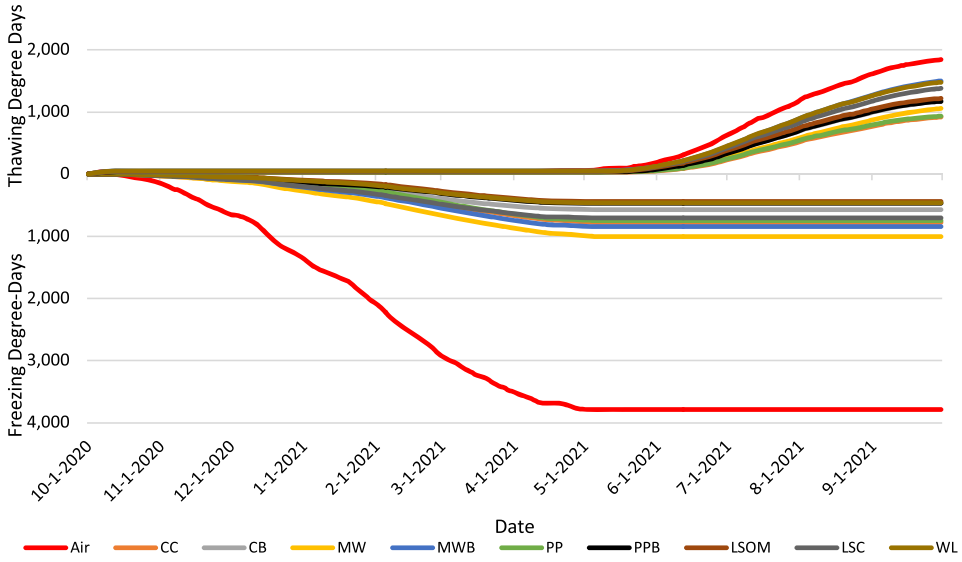

**Fig. 5.** (A) Modelled MAAT over the study area for 2020/2021. (B) Modelled MAGST ranges over the study area for 2020/2021. (C) Modelled $n_f$ values over the study area for 2020/2021. (D) Modelled $n_t$ values over the study area for 2020/2021. Base map (ESRI), map datum in NAD83.

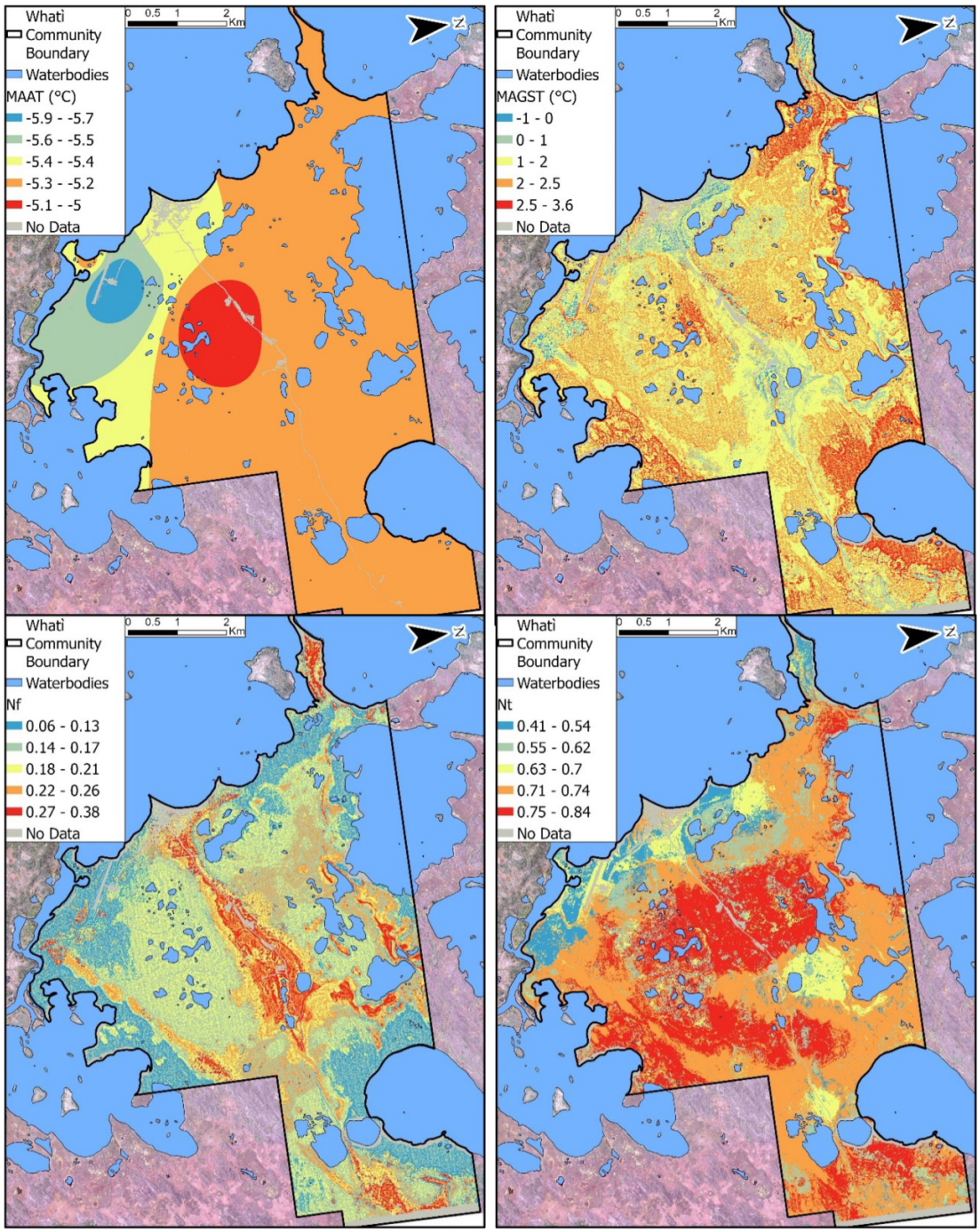


## Model outputs

### MAAT

Modelled MAAT values from October 2020 to October 2021 ranged between −5 °C and −6 °C (Fig. 5A). Seasonally, RMSE was highest in the winter at 0.007 °C and lowest in the summer at 0.0001 °C.

### MAGST

Modelled MAGST values from October 2020 to October 2021 ranged from −1 °C to 3.5 °C (Fig. 5B). Seasonally, RMSE was highest in the spring and summer at 1.56 °C and lowest in the fall (0.57 °C). Winter was similar to spring and summer at 1.54 °C. The average difference for all the ground sensors came out to be −1.65 °C when measured results were sub-

**Fig. 6.** Average temperature and temperature ranges for the TTOP and MAGST surfaces for different vegetation classes.

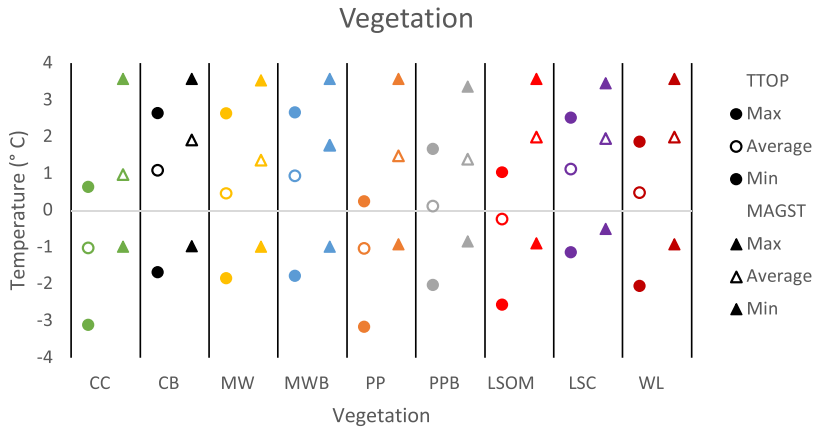


tracted from modelled temperatures. Each vegetation class had similar temperature ranges, with the lowest temperatures found in mix-wooded forests and mix-wooded forest burnt (−0.98 °C) and the highest in mix-wooded forest burnt and low-shrub organic matter (3.58 °C) (Fig. 6). Average temperatures ranged from 1.38 °C in mix-wooded forest to 1.92 °C in coniferous forest and low-shrub clearing (Fig. 5B).

### $n_t$ and $n_f$

Modelled $n_f$ values ranged from 0.05 to 0.383, with an average value of 0.17 (Fig. 5C). Vegetation classes with higher organic material such as peat plateau, peat plateau burnt, and low-shrub organic matter had lower average $n_f$ values (0.16), while classes with less organic matter such as mix-wooded forests and mix-wooded forests burnt had higher average $n_f$ values of 0.19 and 0.21. Modelled $n_t$ values range from 0.4 to 0.84, with an average value of 0.7 (Fig. 5D). This is a much higher value than $n_f$. Coniferous forest, peat plateau burnt, and peat plateau have the lowest $n_t$ values (0.55, 0.58, and 0.61). The rest of the vegetation classes were all around 0.7.

### TTOP model

Modelled TTOP from October 2020 to October 2021 ranged from −3.2 °C to 2.7 °C across the study area (Fig. 7). TTOP had an average of 0.32 °C, with 31% of the surface being classified as permafrost (having a TTOP ≤ 0 °C) and 69% as non-permafrost (>0 °C). Peat plateaus, coniferous forests, and low-shrub organic matter had the highest percentage of the ground being underlain by permafrost (99.7%, 96%, and 71.6%). Coniferous forest burnt and low-shrub clearing had the lowest percentage of permafrost (3.8% and 4.4%). TTOP temperatures decrease with increasing elevation. Areas with an elevation below 246.8 m a.s.l have an average temperature of 0.68 °C, whereas areas between 261.9 m and 282.7 m a.s.l have an average temperature of −0.29 °C. A similar trend is observed in the relationship with TPI, as <−0.8 had an average temperature of 0.69 °C and 1.1–8.9 had an average temperature of −0.87 °C. Results show that low TTOP correlates with low MAGST and high $n_f$ (Figs. 5 and 7). This is similar to the results found in Garibaldi et al. (2021).

## TTOP and MAGST comparison

Breaking down TTOP and MAGST, vegetation classes with high organic matter had the highest difference in average temperature between the TTOP and MAGST surfaces. This included peat plateau (−2.52 °C), low-shrub organic matter (−2.23), and coniferous forest (−1.99 °C). Whereas fire-disturbed areas and areas with low organic matter had the lowest differences between average temperature, burnt coniferous forest, burnt mix-wooded forest, low-shrub clearing, and mixed-wooded forest (−0.81 °C, −0.83 °C, −0.83 °C, and −0.9 °C). Vegetation classes in MAGST range from 0.97 °C (coniferous forest) to 2 °C (wetland). Maximum MAGST ranges from 3.37 °C (peat plateau) to 3.58 °C (mix-wooded forest burnt and wetland). Minimum MAGST also stays consistent with variable vegetation ranging from −0.98 (coniferous forest, mixed-wooded forests, and mixed-wooded forests burnt) to −0.5 °C (low-shrub clearing). Variations by vegetation class are greater on the TTOP surface. Average temperatures range from 0.24 °C (peat plateau) to 2.66 °C (mix-wooded forest burnt). Maximum temperatures range from −1.04 °C (peat plateau) to 1.12 °C (low-shrub clearing). Minimum temperatures have a similar result, ranging from −3.16 °C (peat plateau) to −1.14 °C (low-shrub clearing) (Fig. 6). Elevation shows a general trend of decreasing temperature with an increase in elevation. TPI shows a trend of warmer temperatures in hollows (−0.8) and cooler temperatures on peaks and ridges (8.9). This is observed on both the TTOP surface and the MAGST surface (Figs. 8 and 9).

## TTOP accuracy assessment

There were 139 CAS sites, and 136 fell within the modelled study area (Table 2). The TTOP model agreed with 85 out of 136 of the CAS, or 62.5%, meaning that 51 (37.5%) did not agree. The ecosystem classifications that agreed the most with the CAS classifications were peat plateau, coniferous forest, and mix-wooded forest burnt (16/16 [100%], 16/19 [84%], and 10/12 [83%]). Ecosystem classifications that agreed

**Fig. 7.** Modelled TTOP for the study area in 2020/2021. Base map (ESRI), map datum in NAD83.

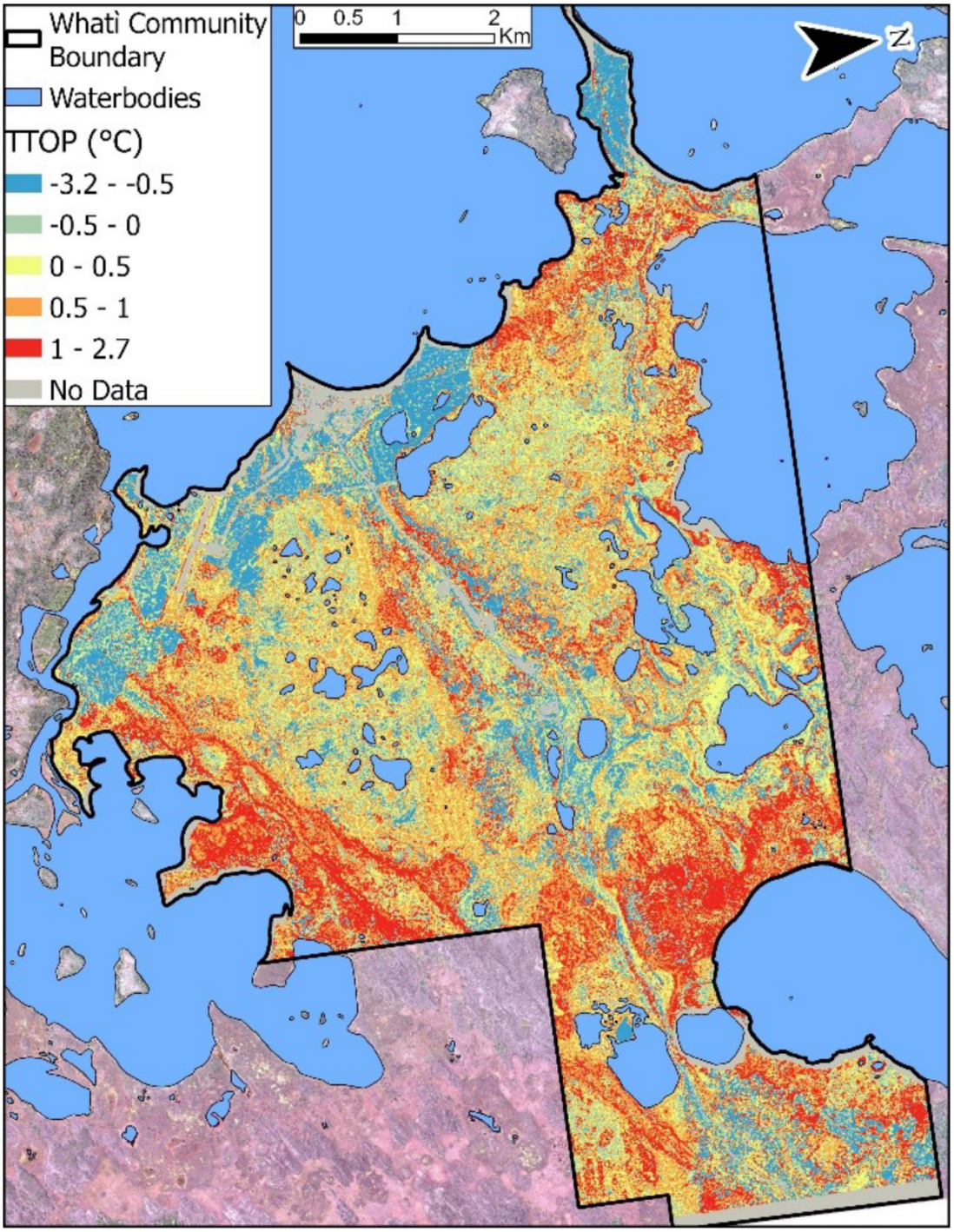




the least were low-shrub organic matter and low-shrub clearing (2/9 [22%] and 4/10 [40%]) (Figs. 10 and 11). Nineteen out of 136 [14%] of CAS were deemed false positive, meaning that the TTOP model indicated permafrost when it was not present. This primarily occurred in wetlands, mixed-wooded forests, and low-shrub clearings (38%, 29%, and 50%). Thirty-two out of 136 (23.5%) were deemed false negative, meaning that the TTOP model indicated no permafrost when permafrost was present. This primarily occurred in peat plateau burnt, low-shrub organic matter, and coniferous forest burnt (58%, 56%, and 36%, respectively). RMSE was calculated for five of the sensors that had a full year of TTOP measurements and showed a value of 1.2 °C.

## Seasonal frost and permafrost model

A seasonal frost model ($TTOP_{SF}$) was generated from the TTOP surface by identifying cells with TTOP values greater than 0 °C. The seasonal frost model was then run independently for the identified cells and then merged with the non-excluded cells from the TTOP model run (all values ≤0 °C).

**Fig. 8.** Average temperature and temperature ranges for the TTOP and MAGST surfaces for different topographic position index classes.

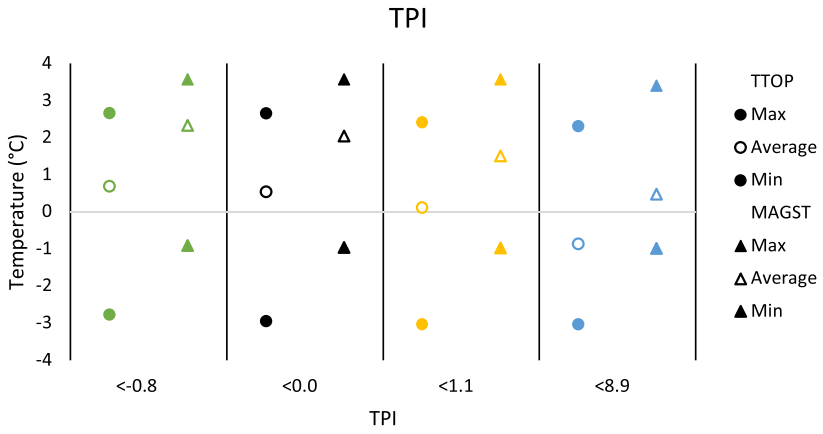


**Fig. 9.** Average temperature and temperature ranges for the TTOP and MAGST surfaces for different elevation classes.

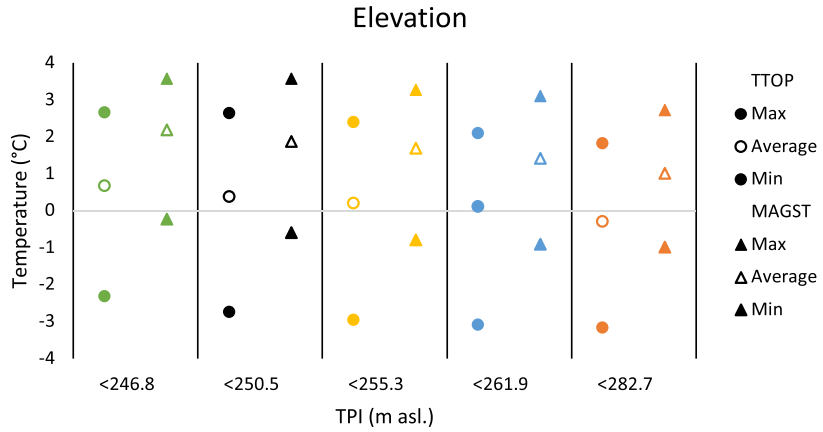


This generated a surface with a temperature range of −3.2 °C to 3.3 °C and an average temperature of 0.55 °C, which is 0.23 °C higher than the TTOP model (Fig. 12). In the region, 28% was underlain with permafrost. This is 3% less than the TTOP surface. The accuracy assessment run on the TTOP surface was also run on the $TTOP_{SF}$ surface, yielding identical results.

## Discussion

### Temperature typicality

The TTOP model is an equilibrium model and therefore is most accurate when applied during stable and equilibrium thermal conditions in the air and ground (Wright et al. 2003; Riseborough 2007; Garibaldi et al. 2021). However, this concept is ideal and may not hold true under current conditions as much of the planet, especially in permafrost regions, is rapidly warming (Osterkamp and Romanovsky 1999; Vitt et al. 2000; Stuenzi et al. 2021). As a result, it is challenging to apply the TTOP model in remote areas where long-term temperature data does not exist. In instances where limited data are available due to remoteness, temperature typicality has been used to show that conditions in the data collection period are representative of longer term averages (e.g., Garibaldi et al. 2021). Although there has been evidence showing recent warming air temperature trends, the data was collected during a relatively cold year compared to the recent average. The TTOP surface data was collected during a period of air temperature within the standard deviation of a 50-year average; however, the data collection period was colder than the 10-year (2012–2021) average. Because TTOP is an equilibrium model, this colder sampling year is actually advantageous. Often, many studies utilizing TTOP recommend longer data collection periods. Examining the data here shows that a longer study over the last 5 years, not including the data collection year (2020–21), may have actually placed the surface out of equilibrium with historical climate data and led to greater inaccuracies. Although more data over a longer time is always preferred, this study utilized a method (GTN network) of capturing heterogeneity in a way that has only been used to model TTOP recently (Bonnaventure et al. 2017; Garibaldi et al. 2021). Due to the conditions in the year of data collection, we do not feel additional data would have drastically changed the outcome of the results or the conclusions on the usability of TTOP in boreal wetland environments. It must be stated,

**Fig. 10.** Accuracy assessment output comparing the TTOP model with cryotic assessment sites (CAS) (Daly et al. 2022) overlaying vegetation surface. Accuracy assessment: graph showing the number of true, false positive, and false negative sites for each vegetation class. Base map (ESRI), map datum in NAD83.

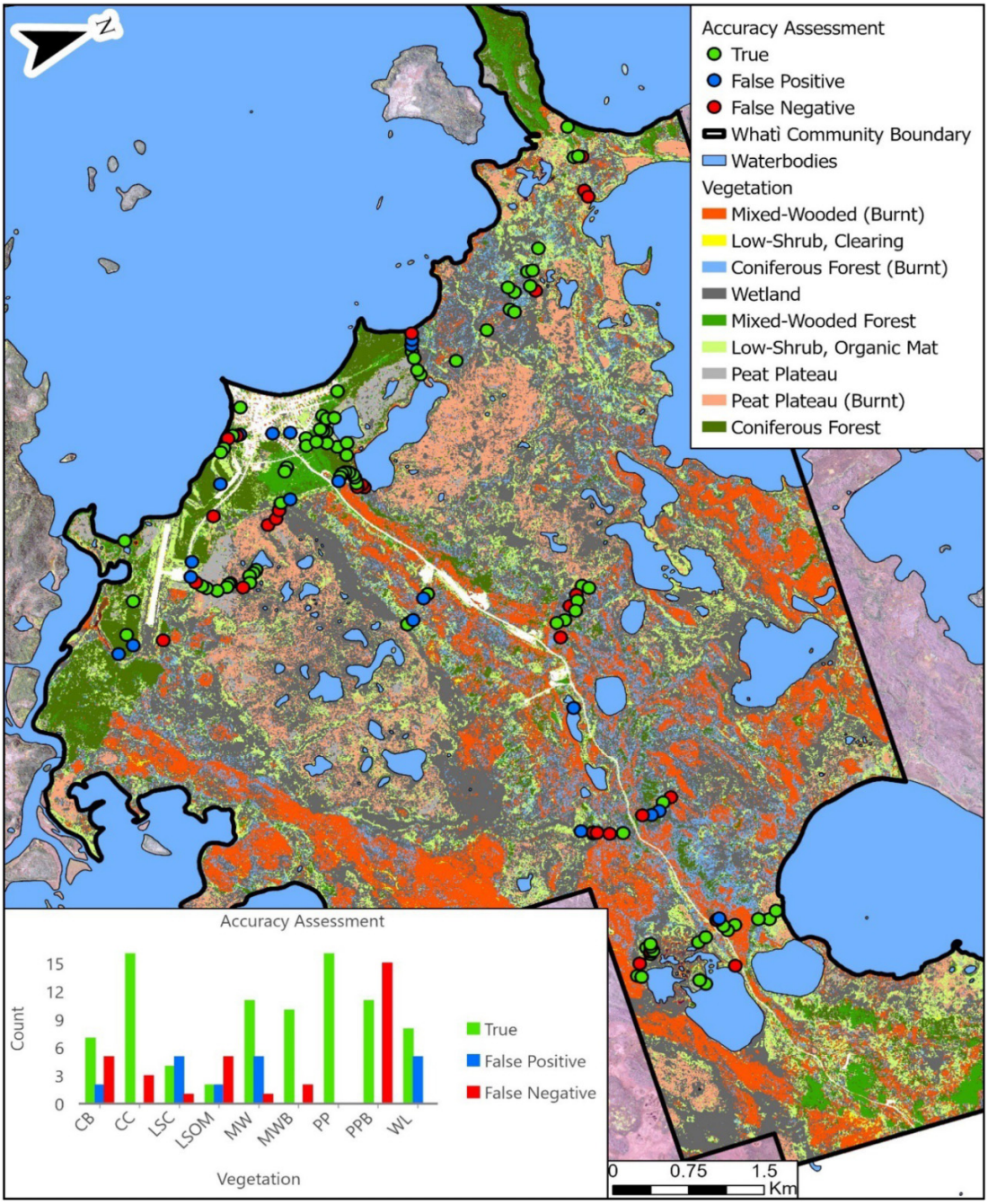


however, that caution must be used in relying strictly on the TTOP model for short datasets and that temperature analysis and typicality must be conducted. If the study had been conducted in a year that was deemed untypical (warmer or colder), the GTN network should still be able to capture the heterogeneity of the surface temperature. This is based on the idea that typically portions of the landscape that are prone to being warmer or colder or accumulating high or low levels of snow cover remain consistent from year to year, even in atypically cold or warm years (Young et al. 1997; Garibaldi et al. 2021). If this study had taken place in a non-typical year, the spatial heterogeneity would still have been captured; however, the value of the results are likely to have been shifted toward the warmer or colder end of the spectrum.

## TTOP and binary logistic regression model comparison

Daly et al. (2022) ran a binary logistic regression (BLR) model for Whatì that utilized 139 CAS recorded in August of 2019 as well as digital surface models to understand the distribution of near-surface permafrost. The BLR model

**Fig. 11.** Study area sections to better show accuracy assessment outcomes. True (Green), false positive (blue), and false negative (red). Base map (ESRI), map datum in NAD83.

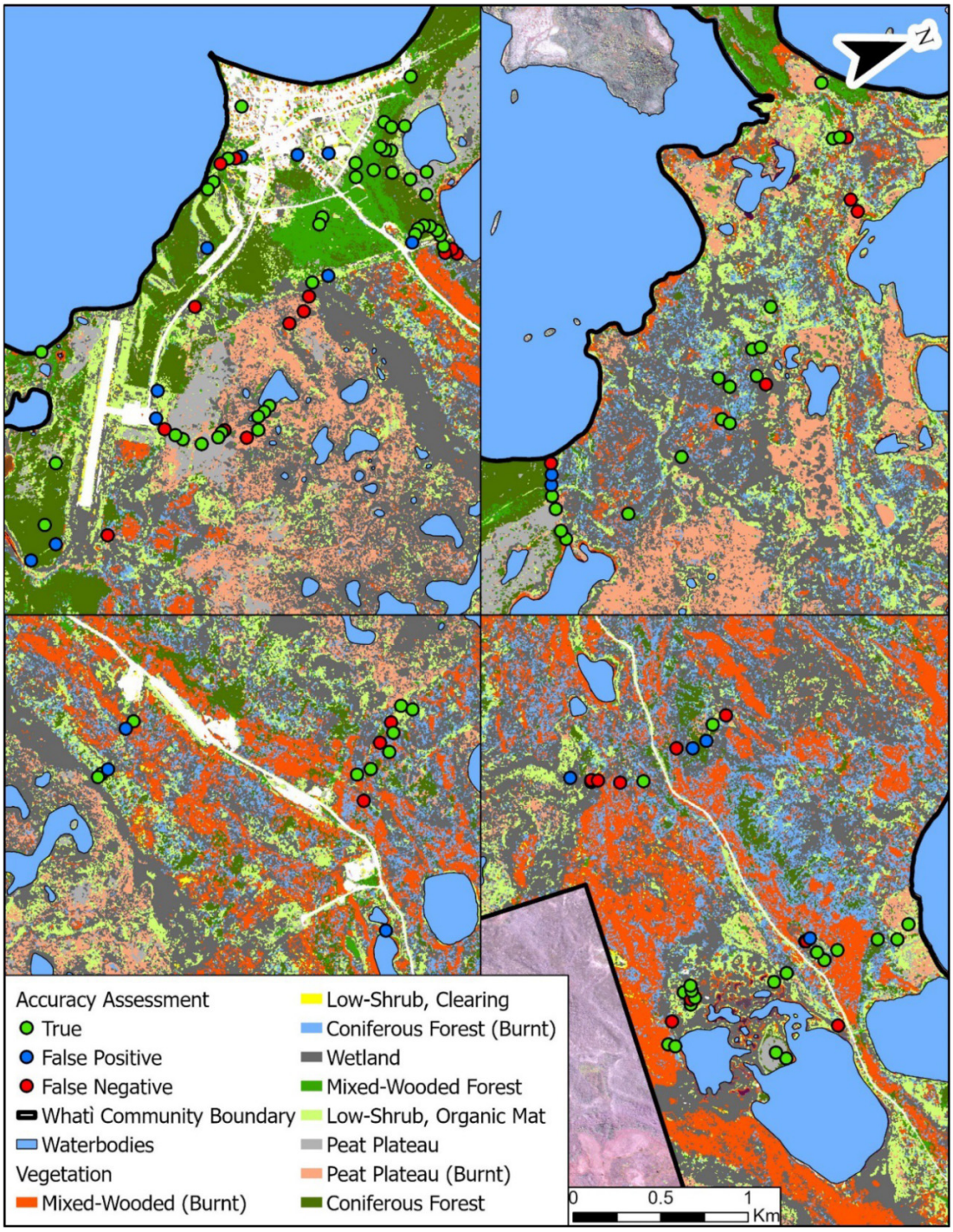


is a probability-based model and defines the overall permafrost amount according to the average of the surface itself (Lewkowicz and Ednie 2004; Bonnaventure and Lewkowicz 2012). The BLR model predicted that 50% or 30 km$^2$ of the study area had a 50% or greater probability of being underlain by near-surface permafrost. The 50%–90% value is consistent with the TTOP results of Obu et al. (2019) in that it is classified within the extensive discontinuous permafrost zone, although with generally lower probability but more variability at higher resolution. Daly et al. (2022) modelled that 36% of the study area had a permafrost probability of 99% or greater. This is similar to the value in the TTOP model conducted in this study.

The TTOP model is a processed-based model with temperature output, defining permafrost as having a temperature at or below 0 °C (Zhang et al. 2000; Obu et al. 2019). In this study, the TTOP model predicted 31% or 18.6 km$^2$ of the study area being underlain with permafrost (TTOP $\leq$ 0 °C), showing

**Fig. 12.** A merged surface of the TTOP model and the seasonal frost model ($TTOP_{SF}$), where the seasonal frost model was run on TTOP grid cells that were greater than 0 °C. Base map (ESRI), map datum in NAD83.

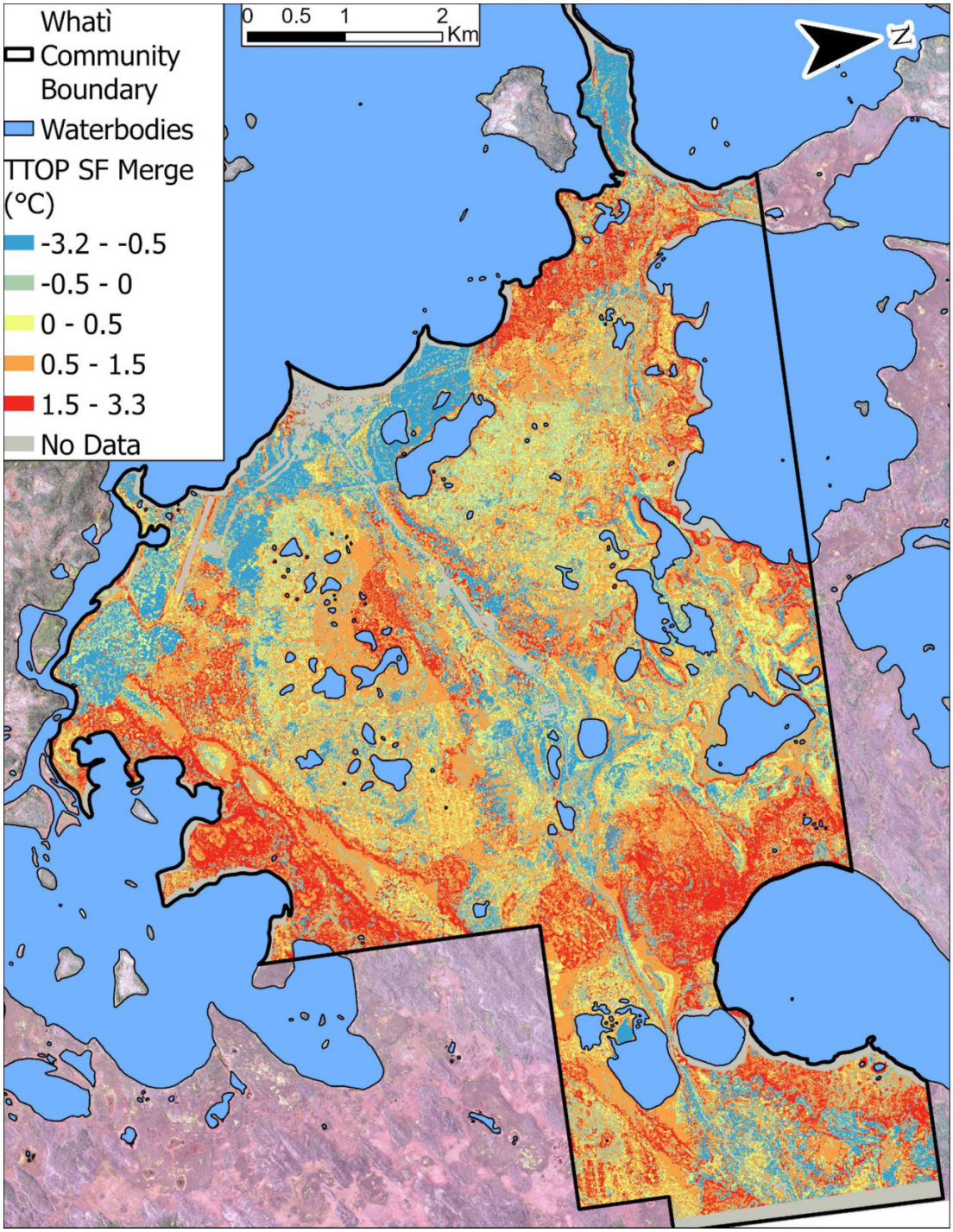




a 19% or 12.4 km$^2$ difference with a 50% probability and a 7% difference with a 99% probability. This variation between the two models can be a product of differences with respect to output or the way permafrost is defined. Utilizing the TTOP approach, there is a firm cutoff (0 °C), and thus the two are not as directly comparable as it might first seem. As an example, if a more liberal definition of TTOP is given (e.g., TTOP $\leq$ 0.5 °C) when examining the overall permafrost amount, the percentage underlain by permafrost increases drastically to 57%. This shows that these models could be more comparable than first anticipated and that the spatial distribution as well as the overall amount of permafrost must be examined before direct comparison.

Vegetation classes where the two models had similar permafrost percentages included peat plateau, coniferous forest, and low-shrub organic matter (Table 3). The vegetation classes that differed the most between the models were peat plateau burnt, low-shrub clearing, mixed-wooded forest burnt, conif-

**Table 3.** The percentage of each vegetation class underlain by permafrost for the TTOP model and the BLR model, and the area proportion for each class.

| Vegetation class | TTOP (%) | BLR (%) | Study area (%) |
|---|---|---|---|
| Coniferous forest (CC) | 96 | 100 | 8.3 |
| Coniferous forest burnt (CB) | 3.8 | 34 | 9.2 |
| Mixed-wooded forest (MW) | 2.9 | 17 | 4 |
| Mixed-wooded burnt (MWB) | 7 | 26.1 | 18 |
| Peat plateau (PP) | 99.7 | 99 | 3.2 |
| Peat plateau burnt (PPB) | 38.3 | 99.9 | 8.7 |
| Wetland (WL) | 12.7 | 32.9 | 36.5 |
| Low-shrub organic matter (LSOM) | 71.6 | 71 | 12.7 |
| Low-shrub clearing (LSC) | 4.4 | 3.9 | 0.5 |



erous burnt, and wetland. The other class, mixed-wooded forest, was in the middle. Based on this, it can be understood that the two models had high agreements in areas with high permafrost percentages and vegetation classes with high amounts of organic matter, and as permafrost decreased, so did the agreement between the two models. The TTOP model was much lower in permafrost occurrence in both burnt areas and areas with less amounts of organic matter.

As expected, both the TTOP and BLR models show a decrease in permafrost in burnt ecosystem classes compared to their unburnt counterparts (Burn 1998; Yoshikawa et al. 2002; Holloway et al. 2020). Large discrepancies between the TTOP and BLR models in burnt ecosystems can be attributed to ground surface temperatures warming post-fire while the organic matter present in the ecosystem pre-fire continues to insulate the permafrost beneath it (Shur and Jorgenson 2007; Holloway et al. 2020). Warmer ground surface temperatures are observed in the summer at the GTNs for each of the burnt sites as opposed to their unburnt counterparts. Permafrost in areas with high organic matter tends to be more resilient to forest fires due to higher soil moisture and low drainage properties (Jafarov et al. 2013; Jiang et al. 2015; Holloway and Lewkowicz 2020; Holloway et al. 2020). This can be seen as average summer temperatures increasing by at least 2 °C for each of the burnt ecosystems when compared to their unburnt counterparts. Furthermore, most of the areas with high organic matter contained some amount of *sphagnum* moss, which assists with permafrost preservation post-fire as its thermal conductivity does not change post-burn (Zhang et al. 2015; Holloway and Lewkowicz 2020). Results in Daly et al. (2022) indicate an increase in active layer thickness between peat plateau and peat plateau burnt. However, they also indicate a very small increase in permafrost probability between peat plateau and peat plateau burnt (99% and 99.9%). Permafrost is still present in this ecosystem, as burning did not thaw permafrost but rather simply placed it farther from equilibrium. Thus, if climatic conditions warm at a faster rate than the reestablishment of the permafrost-favourable boreal ecosystem, loss of permafrost is likely (e.g., Smith et al. 2015). Although removal of the surface layer by fire was relatively recent (2014), near-surface permafrost is still present and thus was recorded in the CAS. This explains the inconsistency between the BLR model and the TTOP model and why permafrost is better predicted using the BLR model in this case. Historically, peat plateaus that have been affected by a forest fire have lost permafrost based on burn severity and generally 5–10 years post-fire (Jafarov et al. 2013; Alexander et al. 2018; Holloway et al. 2020).

## Accuracy assessment

The accuracy assessment shows that the TTOP model is more like the CAS ground truthing pits than it is to the BLR model when comparing the percentage of CAS pits that detected permafrost to the percentage of permafrost coverage by the ecosystem. The average difference for each ecosystem type between the TTOP model and the CAS ground truthing pits is 16%, while the average difference between the TTOP model and the BLR model is 19.5%. When burnt ecosystem classes are removed (coniferous burnt, peat plateau burnt, and mixed-wooded forest burnt), those differences go down to 4.7% and 10.7%. These differences can be attributed to the increase in GTN temperatures for burnt ecosystems in both winter and summer.

When broken down by ecosystem, the accuracy assessment showed results like the BLR model comparison, as areas with high amounts of organic matter like peat plateaus and coniferous forests had high accuracy rates (100% and 84%). 100% of the CAS in these ecosystems had permafrost. Another ecosystem with high accuracy was mixed-wooded forest burnt (83%). Only 2/12 (16.7%) of the CAS in this ecosystem had permafrost. This is only a 9% difference from the TTOP estimation of 7%. Most false negative occurrences were in peat plateau burnt ecosystems. This once again can be attributed to an increase in surface temperature post-fire while the thermal conductivity of the ecosystem remains similar to pre-fire conditions (Holloway et al. 2020). False positives were primarily found in wetlands, low-shrub clearings, and mixed-wooded forests. This is attributed to the model not being sensitive enough to the permafrost limiting factors in the ecosystem. These include higher amounts of soil moisture, not allowing the ground to warm enough in the summer, or giving a temperature high enough for the model to be greater than 0 °C. Due to latent heat, these wetter areas are able to dissipate more energy than drier areas (Riseborough 1990). Poorly drained soils tend to have much higher thermal conductivities when frozen in winter than when unfrozen in summer (Romanovsky and Osterkamp 1995). This can cause rapid heat

loss in the winter and slower warming in the summer, leading to a greater thermal gradient between the ground surface and TTOP (Romanovsky and Osterkamp 1995; Jorgenson et al. 2010; Daly et al. 2022).

As the TTOP model is widely used in regional and continental scale models across Canada and all over the world (Smith and Riseborough 2002; Way and Lewkowicz 2016; Bonnaventure et al. 2017; Kukkonen et al. 2020; Garibaldi et al. 2021), it was the primary model used in this study. An alternative model, the seasonal frost model, was also explored for areas where the TTOP model was identified as being greater than 0 °C. When using this model in conjunction with the TTOP model, the average temperature increases to 0.5 °C, 0.2 °C higher than the TTOP model. However, for areas above 0 °C, when subtracting the seasonal frost model from the TTOP model, the average difference is 1 °C, showing that the majority of TTOP are greater than seasonal frost temperatures and that the TTOP model is sufficient for this study area.

## Comparison to other TTOP models

Due to the simplicity and low input requirements of the TTOP model, it has been utilized to generate high-resolution maps (<1 km) (Smith and Riseborough 2002; Juliussen and Humlum 2007; Way and Lewkowicz 2016; Bonnaventure et al. 2017; Obu et al. 2019; Garibaldi et al. 2021). Larger scale models can produce inaccuracies as local variations in vegetation, topography, snow cover, and soil can produce temperature variations of several degrees in MAGT over a small area (Judge 1973; Smith and Riseborough 2002). Obu et al. (2019) use remotely sensed data as inputs to the TTOP model to generate a 1 km × 1 km permafrost temperature and zonation map for the entire Northern hemisphere. In this model, permafrost is defined as an area with a MAGT below 0 °C (Zhang 2005). It modelled that the region surrounding Whatì has a MAGT of −2 °C to −1 °C and falls into the discontinuous permafrost zone, being 50%–90% underlain by permafrost. Using a 1 km$^2$ resolution in this study area would break it up into 60 parts, leading to a generalization of the model inputs it uses (land surface temperature, vegetation cover, wetness, and precipitation). This study has shown that the vegetation and DEM variables in this model are so heterogeneous that 1 km$^2$ resolution is not high enough for an accurate study of permafrost presence.

The map produced by Heginbottom et al. (1995) shows the distribution and boundaries of permafrost and ground ice in Canada. The map is produced on a national scale (1:7 500 000) and depicts similar results to the Obu et al. (2019) product. It indicates that Whatì falls into the discontinuous permafrost zone (50%–90% permafrost coverage) and has a MAGT of 0 °C to −2 °C with low ground ice. Similarly, Henry and Smith (2001) produced a ground temperature map of Canada with a resolution of 10 km × 10 km and found that the region of Whatì had a MAGT of 0 °C to −2 °C. Smith and Riseborough (2002) ran the TTOP model on a national scale to map limiting conditions on permafrost zones in Canada, also placing TTOP in Whatì in the discontinuous permafrost zone (50%–90% permafrost coverage). Like Obu et al. (2019), the maps produced by Heginbottom et al. (1995), Henry and Smith (2000), and Smith and Riseborough (2002) are on a national scale and are able to map out the general trends of MAGT and permafrost distribution in Canada but are not able to account for the heterogeneity of boreal landscapes.

High-resolution TTOP models have been shown to have similar errors in a study conducted by Way and Lewkowicz (2016). Their model failed to predict permafrost, which was known to occur in palsa fields. The study claims that one of the reasons this occurs may be due to the fact that the palsas are out of thermal equilibrium with the recent climate (Riseborough 2007), much like the permafrost in boreal peat plateaus. The permafrost in these palsas could be considered climate-driven ecosystem-modified or ecosystem-protected (Shur and Jorgenson 2007). The study agrees with Riseborough (2007), which shows that the TTOP model can fail in transient conditions associated with long-term climate trends. This shows a positive bias near the permafrost-seasonal frost boundary. As the TTOP model is climate-based, high-resolution studies may be better suited to model MAGT for permafrost that is climate-driven. This primarily occurs in the High Arctic. It has shown that it can accurately model ground temperature variability in the High Arctic (Bonnaventure et al. 2017; Garibaldi et al. 2021), and it consequently assists with explaining ground temperature drivers. This study has found that permafrost in Whatì is climate-driven ecosystem-modified, affecting the usefulness of the TTOP model here.

## Disturbed vs. undisturbed regions

Forest fire frequency and severity have and are expected to increase with climate change in boreal forest regions (Kasischke and Turetsky 2006; Wotton et al. 2010; Wang et al. 2015). Forest fires affect the energy balance and thermal conductivity of the ground by altering or decreasing the thickness of the organic layer, changing the albedo, and increasing the total solar radiation reaching the surface as well as the snow cover (Yoshikawa et al. 2002; Jorgenson et al. 2010; Holloway et al. 2020). Therefore, it is important to understand its implications for permafrost presence and degradation. Fire can increase surface and soil temperatures in boreal forests immediately following the fire and lasting decades later (Yoshikawa et al. 2002; O'Donnell et al. 2011; Nossov et al. 2013; Zhang et al. 2015; Gibson et al. 2018; Li et al. 2021). The community of Whatì was impacted by a fire in 2014, burning roughly 84% of the study area (Daly et al. 2022). This study was conducted during the period of maximum active layer thickness, which generally occurs 5–10 years post-fire (Yoshikawa et al. 2002). The temperature increase is observed in the TTOP model between the three ecosystems, where both burnt and unburnt regions can be directly compared. In coniferous forests, there is an average MAGT increase of 2.1 °C; in peat plateau, there is an increase of 1.1 °C; and in mixwooded forests, there is an increase of 0.46 °C. The increase in temperatures can be part of the reason why results in the TTOP model showed a decreasing presence of permafrost for burnt areas in comparison to the BLR model and CAS sites. However, these surface temperature increases seem to have had minimal effects on the permafrost presence of the peat

plateau burnt CAS sites. This is due to peatlands being more resistant to burning because of their high moisture and latent heat contents (Jafarov et al. 2013; Daly et al. 2022). The coniferous forest, however, had a large difference between burnt and unburnt sites for both the TTOP model and CAS sites. A burnt forest loses its tree canopy and thus its ability to intercept snow (Holloway et al. 2020), leading to a deeper snowpack, greater insolation, and a lower $n_f$. This, combined with a decreased organic layer and albedo, can cause permafrost loss (Jafarov et al. 2013; Smith et al. 2015; Holloway et al. 2020). The study illustrated that the greater the amount of disturbance, the more difficult it is for an area to be modelled by TTOP. This idea is shown in the number of false negatives that occurred in disturbed areas, regardless of the original vegetation type.

### Practicality and perturbment for climate change

As areas of high latitude are currently experiencing rapid temperature warming, permafrost thaw in Arctic and boreal regions is expected to increase (Jorgenson et al. 2001; Serreze and Barry 2011; Garibaldi et al. 2021; Swanson et al. 2021). An advantage of the TTOP model over the BLR model and why this study was conducted is its ability to be modified to model the change in permafrost distribution with climate change. Annual data from ClimateNa (AdaptWest 2015; Wang et al. 2016) use climate change projections for various MAAT scenarios for future years (Wang et al. 2016). These scenarios will alter the TDD and FDD of the ground surface within the study area, and inputting that into the TTOP model can give modelled insight into future ground temperatures. They will allow the study to understand how permafrost under different ecosystems will respond to warming ground temperatures under equilibrium conditions.

The effect climate has on permafrost will vary depending on a region's topography, soil type, moisture, vegetation, and snow (Jorgenson et al. 2010). Combining the results of this study with the CAS from Daly et al. (2022), it has been shown that organic matter and soil moisture in these boreal regions develop MAGT that is cooler than MAGST, consistent with what was found in Jorgensen et al. (2010). In this study, they indicate that the thickness of organic matter and moisture have a major effect on MAGT. Allowing permafrost in ecosystems with these characteristics to be more resilient to climate change.

### Uncertainty, improvements, and future work

The limitations and uncertainties in this study result from the TTOP model being an equilibrium model. Even though it has proved to be successful in other regions and on other scales (Bonnaventure and Lewkowicz 2008; Way and Lewkowicz 2016; Obu et al. 2019; Garibaldi et al. 2021), inaccuracies can be attributed to permafrost in peat-rich areas being out of equilibrium with the current climate and temperature. In some instances, the 2 m × 2 m vegetation classification did not match the ecosystem noted in the field. In cases where field stations and GTNs were placed, the vegetation classification was edited, but it still may contain inaccuracies. The model also omits certain metrics that may assist in a more accurate output; adding surficial data or other additional metrics and sensors that collect data on soil moisture, organic layer thickness, and snow depth could play a larger role in improving the accuracy of the model rather than increasing the length of the study.

Future work on this study could involve implementing these metrics into the model to see if they affect MAGT and permafrost distribution. This study could also be combined with the research conducted by Daly et al. (2022) in northern communities in different regions, such as Fort McPherson or Inuvik.

## Conclusion

This study demonstrates that a climatically driven TTOP model is potentially a poor predictor of near-surface permafrost in a disturbed boreal wetland forest environment and should be verified or tested using ground truthing techniques. The model can be used to illustrate the heterogeneity of ground temperature in this environment. It shows that permafrost presence in a boreal wetland ecosystem is not solely climate-dependent, with distribution relying heavily on the heterogeneous nature of the ecosystem. The TTOP model was found to have a 62.5% accuracy rate with most inaccuracies found in burnt regions where permafrost was present but out of equilibrium with the current ground temperatures. The heterogeneity of the vegetation, TPI, and elevation allow for considerable variation in the ground surface and TTOP throughout the study area, ranging from −1 °C to 2.6 °C and −3.2 °C to 2.7 °C. Areas with thick amounts of organic matter are found to have the lowest TTOP, while areas that underwent natural or artificial disturbances have a higher TTOP. The following conclusions can be drawn from this study:

- The assessment of temperature typicality is essential for a TTOP model driven by short-term climate data. As most permafrost landscapes are not in climatological equilibrium, unseasonably warm or cold years can skew the model results. Establishing typicality allows for spatial heterogeneity to be examined even with a temporally short dataset.
- The high-resolution TTOP model in this study was applied to estimate the amount of permafrost in this region (<0 °C) to be 30%. This is a lower estimation compared to coarser resolution TTOP models that cover a larger region, which estimate 50%–90% permafrost coverage utilizing the same permafrost classification method. When compared to the Whatì BLR model that utilized cryotic assessment sites (CAS), 50% permafrost cover was estimated, with 36% of the area having >99% probability of permafrost. Although these models are not directly comparable, this highlights the potential drawbacks of utilizing a climatically driven model to map near-surface permafrost in a time of climate warming. It is thus likely that more permafrost is present around Whatì, which the TTOP approach is not sensitive enough to detect without calibration by ground truthing using CAS.
- Discrepancies and inaccuracies in the TTOP model can be attributed to ground temperatures being out of equilibrium with the current air temperatures. This is most evi-

dent in burnt ecosystems, where the ground temperatures are out of equilibrium with the ground surface and air temperatures, causing false negatives to be recorded.
- This study utilized a combination of the TTOP model for permafrost environments and a seasonal frost model for seasonally frozen portions of the study area. The seasonal frost model, an idea that must be considered in warmer periglacial environments, did not yield enough change for it to be an effective tool in this study area.
- Although we feel the TTOP model may not generally be the best approach for modelling permafrost in this boreal wetland area, one advantage is the ability to model permafrost for future climate scenarios. Giving an understanding of how permafrost in different ecosystems will react to warming temperatures under equilibrium scenarios.
- The use of a GTN network is essential for modelling using TTOP. The GTN network captures additional data across ecosystems that would otherwise not be seen, showing the heterogeneous nature of ground temperatures even in areas with mostly uniform air temperatures.

## Variable names

| | |
|---|---|
| BLR | Bilinear regression |
| CAS | Cryotic assessment sites |
| CB | Coniferous forest burnt |
| CC | Coniferous forest |
| DEM | Digital elevation model |
| EBK | Empirical Bayesian Kriging |
| EBKRP | Empirical |
| FDD | Freezing degree days |
| FDDa | Freezing degree days of the air |
| FDDg | Freezing degree days of the ground surface |
| GTN | Ground temperature node |
| IDW | Inverse distance weighting |
| LSC | Low-shrub clearing |
| LSOM | Low-shrub organic matter |
| MAAT | Mean annual air temperature |
| MAGT | Mean annual ground temperature |
| MAGST | Mean annual ground surface temperature |
| MCS | Microclimate station |
| MW | Mixed-wooded forest |
| MWB | Mixed-wooded forest burnt |
| NN | Natural neighbour |
| PF | Permafrost model |
| $n_f$ | Freezing *n*-factor |
| $n_t$ | Thawing *n*-factor |
| NT | Northwest Territories |
| PISR | Potential incoming solar radiation |
| PP | Peat plateau |
| PPB | Peat plateau burnt |
| RH | Relative humidity |
| rk | ratio of thawed to frozen thermal conductivity |
| RMSE | Root mean squared error |
| SF | Seasonal frost model |
| TDD | Thawing degree days |
| TDDa | Thawing degree days of the air |
| TDDg | Thawing degree days of the ground surface |
| TPI | Topographic position index |
| TTOP | Temperature at top of permafrost |
| WL | Wetland |
| WWS | Whatì weather station |

## Acknowledgements

We thank the Community Government of Whatì for their driving role and continued support for the project and acknowledge the Tłı̨chǫ Traditional Territory on which this study took place. Funding for this project was provided by the Climate Change Preparedness in the North Program. We also thank the Natural Sciences and Engineering Research Council (NSERC), the University of Lethbridge, and the Government of Northwest Territories, Geological Survey for funding contributions and research support. WK was supported by the National Science Foundation Graduate Research Fellowship under Grant No. DGE-1144205 and the Vanier Graduate Scholarship. WorldView imagery and DSMs were provided to WK by the Polar Geospatial Center under NSF-OPP awards 1043681, 1559691, and 1542736. We thank Collin Simpson and Aidan Musk for field assistance, and Madeleine Garibaldi and Nick Noad for assistance with data and editing.

## Article information

### History dates
Received: 21 February 2023
Accepted: 6 February 2024
Accepted manuscript online: 8 March 2024
Version of record online: 5 July 2024



### Data availability
The in situ GTN and air sensor data collected in Whatì are available upon request from the corresponding author (philip.bonnaventure@uleth.ca).

## Author information

### Author ORCIDs
Philip P. Bonnaventure https://orcid.org/0000-0002-4157-0689

### Author contributions
Conceptualization: SV, PPB
Formal analysis: SV, PPB
Investigation: PPB
Methodology: PPB
Project administration: PPB
Supervision: PPB
Validation: SD
Writing – original draft: SV, PPB
Writing – review & editing: PPB, SD, WK

## Competing interests

The authors declare there are no competing interests.

# References


AdaptWest. 2015. Gridded current and projected climate data for North America at 1 km resolution, interpolated using the ClimateNA v5. 10 software(T. Wang et al., 2015).

Alexander, H.D., Natali, S.M., Loranty, M.M., Ludwig, S.M., Spektor, V.V., Davydov, S., et al. 2018. Impacts of increased soil burn severity on larch forest regeneration on permafrost soils of far northeastern Siberia. Forest Ecology and Management, **417**: 144–153. doi:10.1016/j.foreco.2018.03.008.

Apps, M., Kurz, W., Luxmoore, R., Nilsson, L., Sedjo, R., Schmidt, R., et al. 1993. Boreal forests and tundra. Water, Air, & Soil Pollution, **70**(1): 39–53. doi:10.1007/BF01104987.

Bonnaventure, P.P., and Lewkowicz, A.G. 2008. Mountain permafrost probability mapping using the BTS method in two climatically dissimilar locations, northwest Canada. Canadian Journal of Earth Sciences, **45**(4): 443–455. doi:10.1139/E08-013.

Bonnaventure, P.P., and Lewkowicz, A.G. 2012. Permafrost probability modeling above and below treeline, Yukon, Canada. Cold Regions Science & Technology, **79–80**: 92–106. doi:10.1016/j.coldregions.2012.03.004.

Bonnaventure, P.P., Lamoureux, S.F., and Favaro, E.A. 2017. Over-winter channel bed temperature regimes generated by contrasting snow accumulation in a high Arctic River. Permafrost and Periglacial Processes, **28**(1): 339–346. doi:10.1002/ppp.1902.

Burn, C.R. 1998. The response (1958–1997) of permafrost and near-surface ground temperatures to forest fire, Takhini River valley, southern Yukon Territory. Canadian Journal of Earth Sciences, **35**(2): 184–199. doi:10.1139/e97-105.

Casagrande, F., Neto, F.A., de Souza, R.B., and Nobre, P. 2021. Polar amplification and ice free conditions under 1.5, 2 and 3 °C of global warming as simulated by CMIP5 and CMIP6 models. Atmosphere, **12**(11): 1494. doi:10.3390/atmos12111494.

Daly, S.V., Bonnaventure, P.P., and Kochtitzky, W. 2022. Influence of ecosystem and disturbance on near-surface permafrost distribution, Whati, Northwest Territories, Canada. Permafrost and Periglacial Processes, **33**(4): 339–352. doi:10.1002/ppp.2160.

Deluigi, N., Lambiel, C., and Kanevski, M. 2017. Data-driven mapping of the potential mountain permafrost distribution. Science of the Total Environment, **590–591**: 370–380. doi:10.1016/j.scitotenv.2017.02.041.

Doré, G., Niu, F., and Brooks, H. 2016. Adaptation methods for transportation infrastructure built on degrading permafrost. Permafrost and Periglacial Processes, **27**(4): 352–364. doi:10.1002/ppp.1919.

Duguay, C.R., Zhang, T., Leverington, D.W., and Romanovsky, V.E. 2005. Satellite remote sensing of permafrost and seasonally frozen ground. Geophysical Monograph-American Geophysical Union, **163**: 91.

Etzelmüller, B., Heggem, E.S.F., Sharkhuu, N., Frauenfelder, R., Kääb, A., and Goulden, C. 2006. Mountain permafrost distribution modelling using a multi-criteria approach in the Hövsgöl area, northern Mongolia. Permafrost and Periglacial Processes, **17**(2): 91–104. doi:10.1002/ppp.554.

Farbrot, H., Etzelmüller, B., Schuler, T.V., Guðmundsson, Á., Eiken, T., Humlum, O., and Björnsson, H. 2007. Thermal characteristics and impact of climate change on mountain permafrost in Iceland. Journal of Geophysical Research: Earth Surface, **112**(F3). doi:10.1029/2006JF000541.

Fisher, J.P., Estop-Aragonés, C., Thierry, A., Charman, D.J., Wolfe, S.A., Hartley, I.P., et al. 2016. The influence of vegetation and soil characteristics on active-layer thickness of permafrost soils in boreal forest. Global change biology, **22**(9): 3127–3140. doi:10.1111/gcb.13248.

Garibaldi, M.C., Bonnaventure, P.P., and Lamoureux, S.F. 2021. Utilizing the TTOP model to understand spatial permafrost temperature variability in a High Arctic landscape, Cape Bounty, Nunavut, Canada. Permafrost and Periglacial Processes, **32**(1): 19–34. doi:10.1002/ppp.2086.

Gibson, C.M., Chasmer, L.E., Thompson, D.K., Quinton, W.L., Flannigan, M.D., and Olefeldt, D. 2018. Wildfire as a major driver of recent permafrost thaw in boreal peatlands. Nature Communications, **9**(1): 1–9. doi:10.1038/s41467-018-05457-1.

Goodrich, L.E. 1982. The influence of snow cover on the ground thermal regime. Canadian Geotechnical Journal, **19**(4): 421–432. doi:10.1139/t82-047.

Heginbottom, J., Dubreuil, M., and Harker, P. 1995. Permafrost map of Canada. The National Atlas of Canada. 5th ed. (1978–1995). Vol. 4177. Natural Resources Canada. Sheet MCR. p. 7.

Helbig, M., Pappas, C., and Sonnentag, O. 2016. Permafrost thaw and wildfire: Equally important drivers of boreal tree cover changes in the Taiga Plains, Canada. Geophysical Research Letters, **43**(4): 1598–1606. doi:10.1002/2015GL067193.

Henry, K., and Smith, M. 2001. A model-based map of ground temperatures for the permafrost regions of Canada. Permafrost and Periglacial Processes, **12**(4): 389–398. doi:10.1002/ppp.399.

Holloway, J.E., and Lewkowicz, A.G. 2020. Half a century of discontinuous permafrost persistence and degradation in western Canada. Permafrost and Periglacial Processes, **31**(1): 85–96. doi:10.1002/ppp.2017.

Holloway, J.E., Lewkowicz, A.G., Douglas, T.A., Li, X., Turetsky, M.R., Baltzer, J.L., and Jin, H. 2020. Impact of wildfire on permafrost landscapes: a review of recent advances and future prospects. Permafrost and Periglacial Processes, **31**(3): 371–382. Available from https://onlinelibrary-wiley-com.ezproxy.uleth.ca/doi/full/10.1002/ppp.2048. doi:10.1002/ppp.2048.

Jafarov, E.E., Romanovsky, V.E., Genet, H., McGuire, A.D., and Marchenko, S.S. 2013. The effects of fire on the thermal stability of permafrost in lowland and upland black spruce forests of interior Alaska in a changing climate. Environmental Research Letters, **8**(3): 035030. doi:10.1088/1748-9326/8/3/035030.

Jenks, G.F. 1967. The data model concept in statistical mapping. International Yearbook of Cartography, **7**: 186–190.

Jiang, Y., Rocha, A.V., O'Donnell, J.A., Drysdale, J.A., Rastetter, E.B., Shaver, G.R., and Zhuang, Q. 2015. Contrasting soil thermal responses to fire in Alaskan tundra and boreal forest. Journal of Geophysical Research: Earth Surface, **120**(2): 363–378. doi:10.1002/2014JF003180.

Jorgenson, M., and Osterkamp, T. 2005. Response of boreal ecosystems to varying modes of permafrost degradation. Canadian Journal of Forest Research, **35**(9): 2100–2111. doi:10.1139/x05-153.

Jorgenson, M.T., Harden, J., Kanevskiy, M., O'Donnell, J., Wickland, K., Ewing, S., et al. 2013. Reorganization of vegetation, hydrology and soil carbon after permafrost degradation across heterogeneous boreal landscapes. Environmental Research Letters, **8**(3): 035017. doi:10.1088/1748-9326/8/3/035017.

Jorgenson, M.T., Racine, C.H., Walters, J.C., and Osterkamp, T.E. 2001. Permafrost degradation and ecological changes associated with a warmingclimate in central Alaska. Climatic Change, **48**(4): 551–579. doi:10.1023/A:1005667424292.

Jorgenson, M.T., Romanovsky, V., Harden, J., Shur, Y., O'Donnell, J., Schuur, E.A., et al. 2010. Resilience and vulnerability of permafrost to climate change. Canadian Journal of Forest Research, **40**(7): 1219–1236. doi:10.1139/X10-060.

Jorgenson, M.T., Romanovsky, V.E., Harden, J.W., Shur, Y.L., O'Donnell, J.A., Schuur, E.A.G., Kanevskiy, M., and Marchenko, S. 2010. Resilience and vulnerability of permafrost to climate change. Canadian Journal of Forest Research, **40**(7): 1219–1236. doi:10.1139/X10-060.

Judge, A. 1973. The prediction of permafrost thicknesses. Canadian Geotechnical Journal, **10**(1): 1–11. doi:10.1139/t73-001.

Juliussen, H., and Humlum, O. 2007. Towards a TTOP ground temperature model for mountainous terrain in central-eastern Norway. Permafrost and Periglacial Processes, **18**(2): 161–184. doi:10.1002/ppp.586.

Karunaratne, K., and Burn, C. 2003. Freezing n-factors in discontinuous permafrost terrain, Takhini River, Yukon Territory, Canada. Paper presented at the Proceedings of the 8th International Conference on Permafrost.

Kasischke, E.S., and Turetsky, M.R. 2006. Recent changes in the fire regime across the North American boreal region—spatial and temporal patterns of burning across Canada and Alaska. Geophysical Research Letters, **33**(9). doi:10.1029/2006GL025677.

Koven, C.D., Riley, W.J., and Stern, A. 2013. Analysis of permafrost thermal dynamics and response to climate change in the CMIP5 earth system models. Journal of Climate, **26**(6): 1877–1900. doi:10.1175/JCLI-D-12-00228.1.

Kukkonen, I.T., Suhonen, E., Ezhova, E., Lappalainen, H., Gennadinik, V., Ponomareva, O., et al. 2020. Observations and modelling of ground temperature evolution in the discontinuous permafrost zone in Nadym, north-west Siberia. Permafrost and Periglacial Processes, **31**(2): 264–280. doi:10.1002/ppp.2040.

Lewkowicz, A.G., and Ednie, M. 2004. Probability mapping of mountain permafrost using the BTS method, Wolf Creek, Yukon Territory, Canada. Permafrost and Periglacial Processes, **15**(1): 67–80. doi:10.1002/ppp.480.

Li, X.-Y., Jin, H.-J., Wang, H.-W., Marchenko, S.S., Shan, W., Luo, D.-L., et al. 2021. Influences of forest fires on the permafrost environment: A review. Advances in Climate Change Research, **12**(1): 48–65. doi:10.1016/j.accre.2021.01.001.

Noh, M.J., and Howat, I. 2017. The Surface Extraction from TIN based Search-space Minimization (SETSM) algorithm Citation DataISPRS. Journal of Photogrammetry and Remote Sensing, ISSN: 0924-2716, **129**: 55–76. doi:10.1016/j.isprsjprs.2017.04.019.

Nossov, D.R., Jorgenson, M.T., Kielland, K., and Kanevskiy, M.Z. 2013. Edaphic and microclimatic controls over permafrost response to fire in interior Alaska. Environmental Research Letters, **8**(3): 035013. doi:10.1088/1748-9326/8/3/035013.

Obu, J., Westermann, S., Bartsch, A., Berdnikov, N., Christiansen, H.H., Dashtseren, A., et al. 2019. Northern Hemisphere permafrost map based on TTOP modelling for 2000–2016 at 1 km$^2$ scale. Earth-Science Reviews, **193**: 299–316. doi:10.1016/j.earscirev.2019.04.023.

Osterkamp, T., and Romanovsky, V. 1999. Evidence for warming and thawing of discontinuous permafrost in Alaska. Permafrost and Periglacial Processes, **10**(1): 17–37. doi:10.1002/(SICI)1099-1530(199901/03)10:1%3c17::AID-PPP303%3e3.0.CO;2-4.

O'Donnell, J., Harden, J.W., McGuire, A.D., and Romanovsky, V. 2011. Exploring the sensitivity of soil carbon dynamics to climate change, fire disturbance and permafrost thaw in a black spruce ecosystem. Biogeosciences, **8**(5): 1367–1382.

O'Neill, H.B., Wolfe, S.A., and Duchesne, C. 2019. New ground ice maps for Canada using a paleogeographic modelling approach. The Cryosphere, **13**(3): 753–773.

Peel, M.C., Finlayson, B.L., and McMahon, T.A. 2007. Updated world map of the Köppen-Geiger climate classification. Hydrology and Earth System Sciences, **11**(5): 1633–1644. doi:10.5194/hess-11-1633-2007.

Riseborough, D. 1990. Soil latent heat as a filter of the climate signal in permafrost. Paper presented at the Proceedings of the Fifth Canadian Permafrost Conference, Collection Nordicana.

Riseborough, D. 2007. The effect of transient conditions on an equilibrium permafrost-climate model. Permafrost and Periglacial Processes, **18**(1): 21–32. doi:10.1002/ppp.579.

Romanovsky, V., and Osterkamp, T. 1995. Interannual variations of the thermal regime of the active layer and near-surface permafrost in northern Alaska. Permafrost and Periglacial Processes, **6**(4): 313–335. doi:10.1002/ppp.3430060404.

Serreze, M.C., and Barry, R.G. 2011. Processes and impacts of Arctic amplification: a research synthesis. Global & Planetary Change, **77**(1/2): 85–96. doi:10.1016/j.gloplacha.2011.03.004.

Shur, Y.L., and Jorgenson, M. 2007. Patterns of permafrost formation and degradation in relation to climate and ecosystems. Permafrost and Periglacial Processes, **18**(1): 7–19. Available from https://onlinelibrary-wiley-com.ezproxy.uleth.ca/doi/abs/10.1002/ppp.582. doi:10.1002/ppp.582.

Smith, M., and Riseborough, D. 1996. Permafrost monitoring and detection of climate change. Permafrost and Periglacial Processes, **7**(4): 301–309. Available from https://onlinelibrary-wiley-com.ezproxy.uleth.ca/doi/abs/10.1002/%28SICI%291099-1530%28199610%297%3A4%3C301%3A%3AAID-PPP231%3E3.0.CO%3B2-R. doi:10.1002/(SICI)1099-1530(199610)7:4%3c301::AID-PPP231%3e3.0.CO;2-R.

Smith, M., and Riseborough, D. 1998. Exploring the limits of permafrost. Paper presented at the Permafrost: Proceedings of 7th International Conference, Yellowknife, Canada.

Smith, M., and Riseborough, D. 2002. Climate and the limits of permafrost: a zonal analysis. Permafrost and Periglacial Processes, **13**(1): 1–15. doi:10.1002/ppp.410.

Smith, S.L., Riseborough, D.W., and Bonnaventure, P.P. 2015. Eighteen year record of forest fire effects on ground thermal regimes and permafrost in the Central Mackenzie Valley, NWT, Canada. Permafrost and Periglacial Processes, **26**(4): 289–303. Available from https://onlinelibrary-wiley-com.ezproxy.uleth.ca/doi/full/10.1002/ppp.1849. doi:10.1002/ppp.1849.

Stuenzi, S.M., Boike, J., Cable, W., Herzschuh, U., Kruse, S., Pestryakova, L.A., et al. 2021. Variability of the surface energy balance in permafrost-underlain boreal forest. Biogeosciences, **18**(2): 343–365. doi:10.5194/bg-18-343-2021.

Swanson, D.K., Sousanes, P.J., and Hill, K. 2021. Increased mean annual temperatures in 2014–2019 indicate permafrost thaw in Alaskan national parks. Arctic, Antarctic, and Alpine Research, **53**(1): 1–19. doi:10.1080/15230430.2020.1859435.

Van Cleve, K., Dyrness, C., Viereck, L., Fox, J., Chapin III, F., and Oechel, W. 1983. Taiga ecosystems in interior Alaska. Bioscience, **33**(1): 39–44. doi:10.2307/1309243.

Vitt, D.H., Halsey, L.A., and Zoltai, S.C. 2000. The changing landscape of Canada's western boreal forest: the current dynamics of permafrost. Canadian Journal of Forest Research, **30**(2): 283–287. doi:10.1139/x99-214.

Walker, X.J., Rogers, B.M., Baltzer, J.L., Cumming, S.G., Day, N.J., Goetz, S.J., et al. 2018. Cross-scale controls on carbon emissions from boreal forest megafires. Global Change Biology, **24**(9): 4251–4265. doi:10.1111/gcb.14287.

Wang, T., Hamann, A., Spittlehouse, D., and Carroll, C. 2016. Locally downscaled and spatially customizable climate data for historical and future periods for North America. PLoS One, **11**(6): e0156720. doi:10.1371/journal.pone.0156720.

Wang, X., Thompson, D.K., Marshall, G.A., Tymstra, C., Carr, R., and Flannigan, M.D. 2015. Increasing frequency of extreme fire weather in Canada with climate change. Climatic Change, **130**(4): 573–586. doi:10.1007/s10584-015-1375-5.

Way, R.G., and Lewkowicz, A.G. 2016. Modelling the spatial distribution of permafrost in Labrador–Ungava using the temperature at the top of permafrost. Canadian Journal of Earth Sciences, **53**(10): 1010–1028. doi:10.1139/cjes-2016-0034.

Way, R.G., and Lewkowicz, A.G. 2018. Environmental controls on ground temperature and permafrost in Labrador, northeast Canada. Permafrost and Periglacial Processes, **29**(2): 73–85. doi:10.1002/ppp.1972.

Weiss, A. 2001. Topographic position and landforms analysis. Paper presented at the Poster presentation, ESRI user conference, San Diego, CA.

Wotton, B.M., Nock, C.A., and Flannigan, M.D. 2010. Forest fire occurrence and climate change in Canada. International Journal of Wildland Fire, **19**(3): 253–271. doi:10.1071/WF09002.

Wright, J., Duchesne, C., and Côté, M. 2003. Regional-scale permafrost mapping using the TTOP ground temperature model. Paper presented at the Proceedings 8th International Conference on Permafrost, Swets and Zeitlinger, Lisse.

Yoshikawa, K., Bolton, W.R., Romanovsky, V.E., Fukuda, M., and Hinzman, L.D. 2002. Impacts of wildfire on the permafrost in the boreal forests of Interior Alaska. Journal of Geophysical Research: Atmospheres, **107**(D1): FFR 4-1–FFR 4-14. doi:10.1029/2001JD000438.

Young, K.L., Woo, M.-k., and Edlund, S.A. 1997. Influence of local topography, soils, and vegetation on microclimate and hydrology at a high Arctic site, Ellesmere Island, Canada. Arctic and Alpine Research, **29**(3): 270–284. doi:10.2307/1552141.

Zhang, T. 2005. Influence of the seasonal snow cover on the ground thermal regime: an overview. Reviews of Geophysics, **43**(4). doi:10.1029/2004RG000157.

Zhang, T., Heginbottom, J., Barry, R.G., and Brown, J. 2000. Further statistics on the distribution of permafrost and ground ice in the Northern Hemisphere. Polar Geography, **24**(2): 126–131. doi:10.1080/10889370009377692.

Zhang, Y., Wolfe, S.A., Morse, P.D., Olthof, I., and Fraser, R.H. 2015. Spatiotemporal impacts of wildfire and climate warming on permafrost across a subarctic region, Canada. Journal of Geophysical Research: Earth Surface, **120**(11): 2338–2356. doi:10.1002/2015JF003679.